CHAPTER 4

4.0 REACTOR

CHAPTER 4
REACTOR

TABLE OF CONTENTS

TABLE OF CONTENTS (continued)

TABLE OF CONTENTS (continued)

TABLE OF CONTENTS (continued)

TABLE OF CONTENTS (continued)

TABLE OF CONTENTS (continued)

CHAPTER 4
REACTOR

LIST OF TABLES

LIST OF FIGURES

4.0 REACTOR

4.1 Summary Description

4.1.1 General Description of Core

The H. B. Robinson Unit 2 (HBR 2) reactor core is comprised of an array of 157 fuel assemblies. The core is cooled and moderated by light water at a normal operating pressure of 2250 psia in the Reactor Coolant System (RCS). The Reactor Coolant System contains boron as a neutron poison. The concentration of boron in the reactor coolant is varied as required to control relatively slow reactivity changes including the effects of fuel burnup.

The reactor core and reactor vessel internals are shown in elevation in Figures 4.1.1-1, 4.1.1-2 and a typical loading pattern is shown in Figure 4.1.1-3.

The HBR 2 reactor core contains 157 fuel assemblies with approximately 67 metric tons of uranium manufactured by AREVA Inc. Each assembly normally contains 204 fuel rod locations (occupied by rods consisting of natural or slightly enriched uranium pellets, solid inert materials or a combination of the aforementioned), twenty rod cluster control (RCC) guide tubes, and one instrumentation tube in a 15 x 15 fuel rod array. The standard fuel rods consist of slightly enriched UO_2 pellets inserted into Zirconium alloy tubes (which are pre-pressurized). If needed, a limited number of zirconium or stainless steel filler rods may be utilized in place of fuel rods. The use of these rods will be in accordance with an approved methodology for analyzing reconstituted fuel (Reference 4.1.1-1). Beginning with Region 11 fuel, integral burnable absorber rods have been used in varying numbers in the core, in the form of rods containing gadolinia (Gd_2O_3) in various concentrations in UO_2, for peaking control and reduction of the BOC critical boron. The RCC guide tubes and the instrumentation tubes are also made of zircaloy. Each assembly contains seven spacers; six of which are located within the active fuel region. In the older design, all of these are bi-metallic. Starting with Region 17 (ANF-11) fuel, only the bottom spacer is bi-metallic, and then with ROB2-28 the bottom spacer is a High Mechanical Performance (HMP™) made of Alloy 718. The rest are a High Thermal Performance (HTP™) all-zircaloy design. There are also three Intermediate Flow Mixer (IFM) grids and a debris-resistant lower tie plate on the HTP™ fuel. The lower tie plate design introduced for Cycle 16 makes use of an array of curved blades to provide a highly efficient debris trap.

There are two features that reduce the fast neutron fluence reaching the pressure vessel wall: axially blanketed fuel, and Part Length Shield Assemblies (PLSAs). The axially blanketed fuel contains a region of natural uranium at the top and at the bottom of each fuel assembly. All gadolinia-bearing pins, prior to Region 20 (ROB-14), contain 12 inches of natural uranium at the top and bottom of the fuel pin, while the non-gad pins contain 6 inches of natural uranium at the top and bottom. Beginning with Region 20 (ROB-14), the gadolinia-bearing pins contain six inches of enriched uranium between six inches of natural uranium at the top and bottom of the fuel rod, and the central gadolinia column. Beginning with Region 34 (ROB2-31), the six inch blanket region of a UO_2 fuel pin contains mid-enriched (2.6%) uranium; the mid-enriched blanket region of a UO_2-Gd_2O_3 fuel pin is 10.5 inches. The PLSAs contain stainless steel inserts in the bottom of each fuel rod and a natural uranium blanket for the top six inches of the active core. The stainless steel inserts at the bottom reduce the active fuel length, but has no effect on the outside dimensions of the assembly.

4.1.2 General Description of Fuel

Figures 4.1.2-1 and 4.1.2-2 depict the fuel assembly interface dimensions for the fuel design which was loaded prior to Cycle 14. Figures 4.1.2-3 and 4.1.2-4 depict the interface dimensions for the HTP^{TM} fuel design. Figures 4.1.2-5 and 4.1.2-6 depict the interface dimensions for the advanced HTP^{TM} fuel design (starting with ROB2-28). Mechanical, thermal-hydraulic and neutronic design values for a typical core loading are shown in Tables 4.1.2-1, 4.1.2-2 and 4.1.2-3, respectively.

The UO_2 (or UO_2 - Gd_2O_3 mixture) is in the form of dished cylindrical pellets made by compacting and sintering the UO_2 (or UO_2 - Gd_2O_3) powder. The pitch of the rods is maintained by seven grid spacers located along the length of the 204 rods. The HTP^{TM} and IFM spacers are welded to the guide tubes; the guide tubes are mechanically attached and secured to the upper and lower tie plates. The instrumentation tube is mechanically captured between the tie plates. Beginning with Region 20 (ROB-14), in addition to being mechanically captured, the instrument tube is welded at the bottom spacer location. Beginning with ROB2-28, the HMP^{TM} spacer is mechanically captured between zircaloy rings welded to the guide tubes. The instrumentation tube is likewise mechanically captured with welded rings at the HMP^{TM} spacer location. The spacers, guide tubes, and tie plates form the structural skeleton of the fuel bundle.

Reload fuel will be similar in physical design to the initial core. The enrichment of reload fuel will be no more than 4.95 + 0.05 (nominal 4.95) weight percent of U-235.

TABLE 4.1.2-1 (page 1 of 3)

MECHANICAL DESIGN VALUES

A. FUEL PELLETS

Initial Enrichment, wt% U-235	0.711 to 4.95
Form	right cylinder
Average UO_2 Density, % Theoretical (through ROB2-27/ROB2-28 and later)	95/96
Pellet Diameter, in.	0.3570

B. FUEL ROD

Number of Rods per Assembly	204
Active Length, in.	144.0 (102.0 for PLSA rod)
Overall Rod Length, in. (through Region 19 (ROB-13)/ Region 20 (ROB-14 through Region 26 (ROB-20)/Region 27 (ROB2-24) ROB 2-25/ROB 2-26 to present)	152.065/151.950/151.978/151.98
Rod Pitch, in.	0.563
Fill Gas	Helium

C. CLADDING

Material (through ROB2-27/ROB2-28 and later)	Zircaloy-4/M5® Alloy
Outside Diameter, in.	0.424
Wall Thickness, in.	0.030

D. FUEL ASSEMBLY

Geometry	15 x 15
Number of Assemblies	157 (12 PLSAs, 145 non-PLSAs)
Fuel Assembly Pitch, in.	8.466
Overall Length, in.	159.71 (excluding upper tie plate leaf spring)

E. CONTROL ROD GUIDE TUBE

Number/Assembly	20
Material	Zircaloy-4
ID, Upper Section, in.	0.511
ID, Dashpot, in.	0.455
Dashpot Length, in.	24.5

F. INSTRUMENTATION TUBE

Number/Assembly	1
Material	Zircaloy-4
ID, in.	0.511

TABLE 4.1.2-1 (page 2 of 3)

G. BI-METALLIC SPACER GRIDS (through ROB2-27)/HMP™ (ROB2-28 and later)

Number per assembly	1
Material	Zircaloy-4 structure with nickel alloy 718 springs/Alloy 718

H. HTP™ SPACER GRIDS

Number per HTP™ assembly	6
Material	Zircaloy-4

I. IFM Grids

Number per HTP™ assembly	3
Material	Zircaloy-4

J. COMPONENT WEIGHTS

Weights per Assembly:	
Fuel	
Through ROB2-27	1093 lb (non-PLSA)
ROB2-28 and later	1101 lb (non-PLSA)
Cladding	
Zircaloy-4 (through ROB2-27)	271.6 lb
M5® (ROB2-28 and later)	269.4 lb
End Caps	
Zircaloy-4 (through ROB2-27)	3.1 lb
M5® (ROB2-28 through ROB2-30)	3.1 lb
Zircaloy-4 (ROB2-31 and later)	3.1 lb
Plenum Spring	
Nickel Alloy X-750	5.95 lb
Bi-metallic Spacers (through ROB2-27)	
Zircaloy-4	1.32 lb (per spacer)
Nickel Alloy 718	0.22 lb (per spacer)
HMP™ Spacer (ROB2-28 and later)	
Nickel Alloy 718	2.4 lb
HTP™ Spacers	
Zircaloy-4 [through Region 23 (ROB-17) / Region 24 (ROB-18) and later]	14.18 lb / 13.67 lb
IFM Spacers	
Zircaloy-4	3.53 lb
Control Rod Guide Tube Assembly	
Zircaloy-4	20.94 lb (through ROB2-27)/26.68 lb (ROB2-28 and later)
Instrument Tube	
Zircaloy-4	1.10 lb
Upper and Lower Tie Plates	
Stainless Steel/Nickel Alloy	25.36 lb
Miscellaneous Cage Components	
Zircaloy-4	0.66 lb (through ROB2-27)/0.22 lb (ROB2-28 and later)
Stainless Steel/Nickel Alloy	0.88 lb

TABLE 4.1.2-1 (page 3 of 3)

Total Assembly Weight	
through Region 23 (ROB-17)	1442.1 lb (Non-PLSA)/
Region 24 (ROB-18) through ROB2-27	1442 lb (Non-PLSA)
ROB2-28 and later	1453 lb (Non-PLSA)
Uranium Weight per Assembly, kg	
through ROB2-27	435.0 (Non-PLSA)
ROB2-28 and later	436-440 (Non-PLSA)

K. INSERT USED WITH PLSA FUEL RODS (ONLY)

Material	304L stainless steel
Diameter, In.	0.350
Length, In.	42.0

Note: The values in Sections J and K are representative of High Thermal Performance (HTP^{TM}) Fuel Assemblies. Standard Mixing Vane (SMV) Fuel Assemblies do not have HTP^{TM} grids or IFM grids but have 7 Bi-Metallic grids.

TABLE 4.1.2-2

THERMAL-HYDRAULIC DESIGN VALUES[1]

Rated Heat Output, Mwt	2339
Heat Generated in Fuel, %	97.4
Nominal Design Pressure, psia	2250
Nominal Inlet Temperature, ºF	547.6
Average Core Temperature, ºF	577.0
Nominal Active Heat Transfer Surface Area, ft^2 [2]	42,662
Total Reactor Coolant Flow, lb/hr	
Maximum	$113.0x10^6$
Nominal	$108.0x10^6$
Minimum	$97.3x10^6$
Maximum Core Bypass Flow, %	5.5
Minimum Active Coolant Flow, lb/hr	$91.9x10^6$

1. Values provided here are for modeling purposes and may be bounding of actual plant values.

2. Active fuel length x cladding perimeter x number of fuel rods, may vary by cycle mix of fuel design.

TABLE 4.1.2-3

TYPICAL NUCLEAR DESIGN VALUES

Cold (68ºF)	
Neutron Multiplication Factor (infinity), k_∞, clean-no Xe or Sm	1.3834
Neutron age, τ, cm^2	34.56
Migration area, M^2, cm^2	37.54
Water-to-Fuel Volume Ratio	1.76
Hot (572ºF), Fuel Temperature = 1200ºF	
Neutron Multiplication Factor (infinity), k_∞, clean-no Xe or Sm	1.3259
Neutron age, τ, cm^2	53.87
Migration area, M^2, cm^2	59.83
Effective Delayed Neutron Fraction, β_{eff}	0.007045
Prompt Neutron Lifetime, μsec	25.26 (1050 ppm)

REFERENCES: SECTION 4.1

4.1.1-1 ANF-90-082(P)(A), "Application of ANF Design Methodology for Fuel Assembly Reconstitution," May 1995.

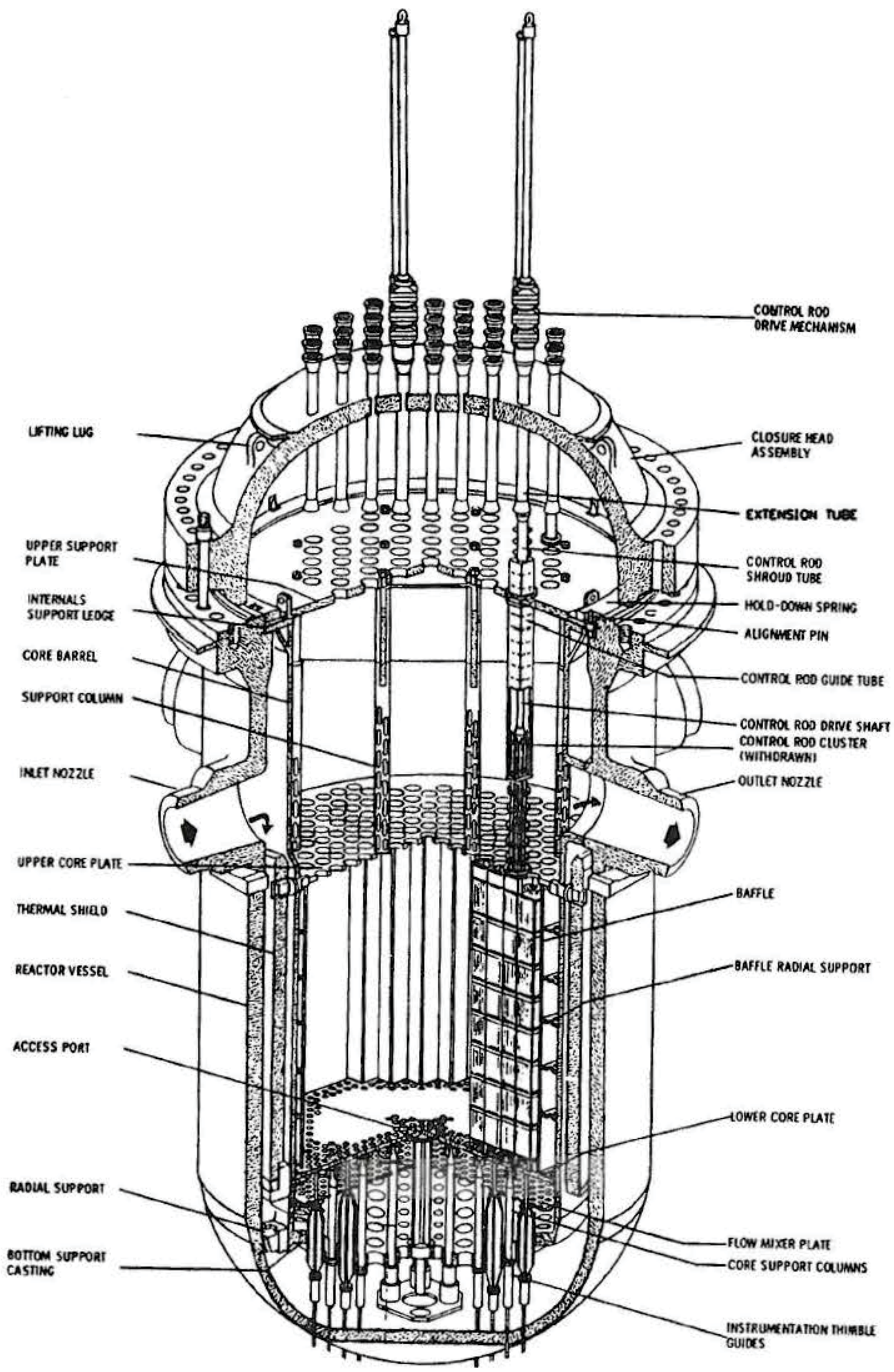

REVISION NO. 21

H. B. ROBINSON UNIT 2 Carolina Power & Light Company UPDATED FINAL SAFETY ANALYSIS REPORT	REACTOR CORE AND REACTOR VESSEL INTERNALS ELEVATION	FIGURE 4.1.1 - 1

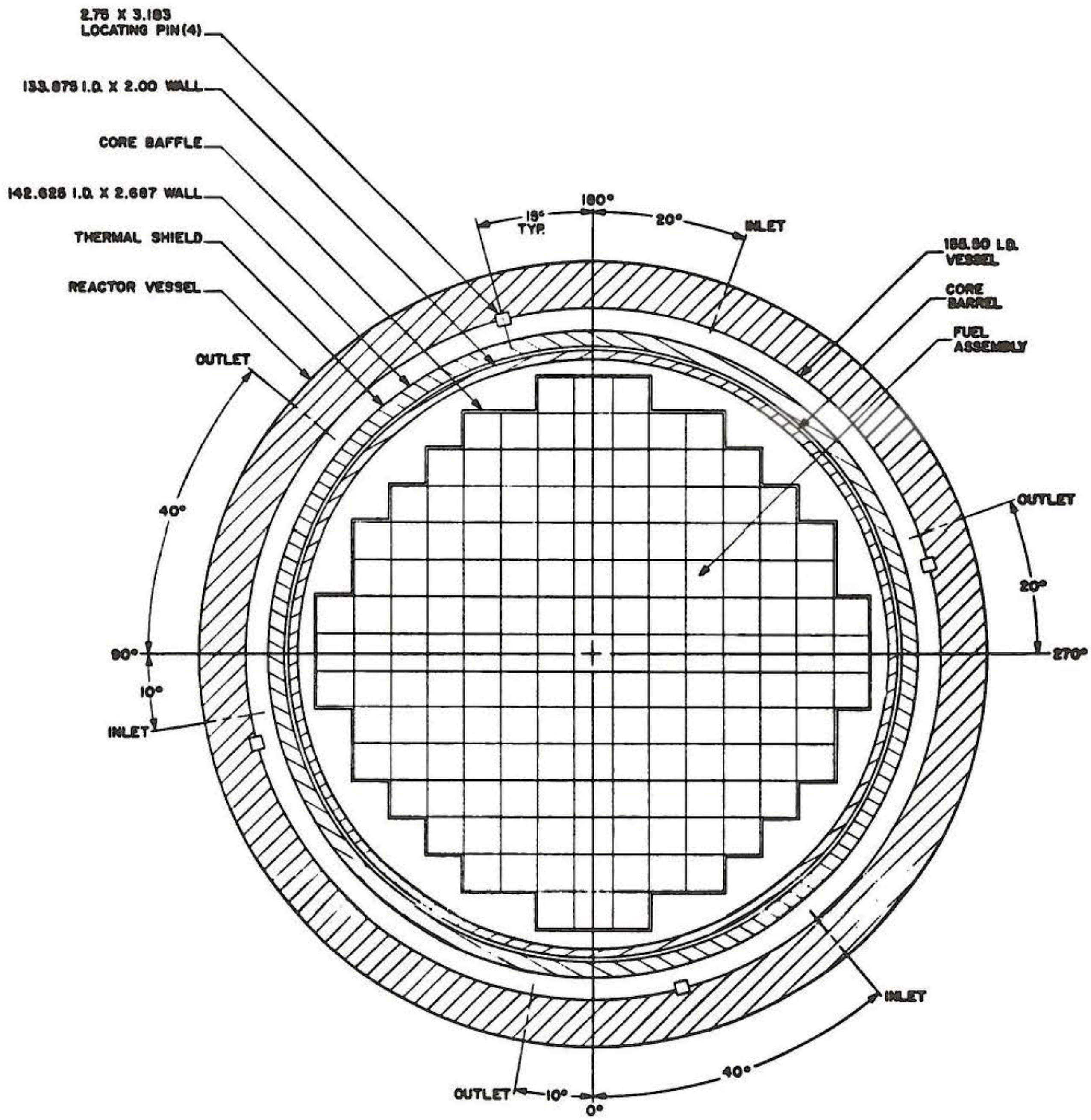

H. B. ROBINSON UNIT 2 Carolina Power & Light Company UPDATED FINAL SAFETY ANALYSIS REPORT	REACTOR CORE AND REACTOR VESSEL INTERNALS CROSS SECTION	FIGURE 4.1.1 - 2

	R	P	N	M	L	K	J	H	G	F	E	D	C	B	A
1							P	P	P						
2					2	2	0	1	0	2	2				
3				2	0	1	1	0	1	1	0	2			
4			2	0	1	0	2	1	2	0	1	0	2		
5		2	0	1	2	2	0	3	0	2	2	1	0	2	
6		2	1	0	2	1	1	0	1	1	2	0	1	2	
7	P	0	1	2	0	1	1	2	1	1	0	2	1	0	P
8	P	1	0	1	3	0	2	2	2	0	3	1	0	1	P
9	P	0	1	2	0	1	1	2	1	1	0	2	1	0	P
10		2	1	0	2	1	1	0	1	1	2	0	1	2	
11		2	0	1	2	2	0	3	0	2	2	1	0	2	
12			2	0	1	0	2	1	2	0	1	0	2		
13				2	0	1	1	0	1	1	0	2			
14					2	2	0	1	0	2	2				
15							P	P	P						

P - Part Length Shield Assembly
0 - Feed Assembly
1 - Once-burned Assembly
2 - Twice-burned Assembly
3 - Thrice-burned Assembly

AMENDMENT NO. 12

H.B. ROBINSON UNIT 2 Carolina Power & Light Company UPDATED FINAL SAFETY ANALYSIS REPORT	TYPICAL LOADING PATTERN	FIGURE 4.1.1-3

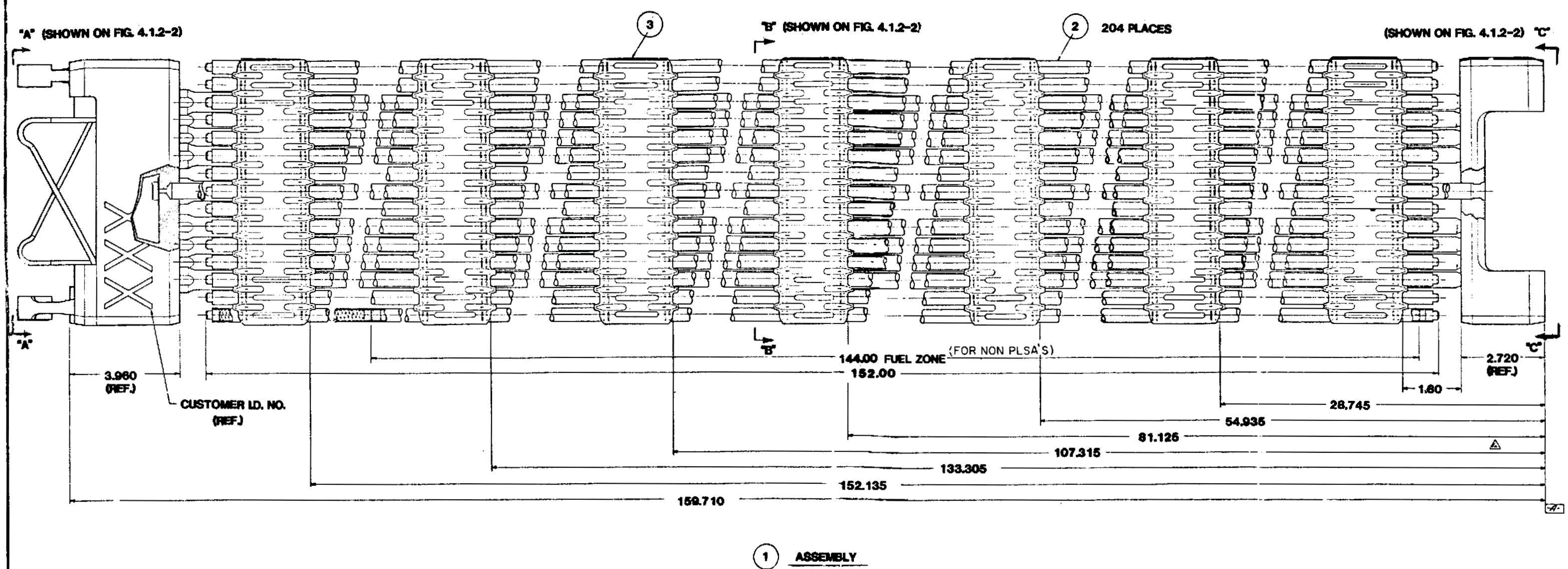

AMENDMENT 3

H. B. ROBINSON
UNIT 2
Carolina Power & Light Company
UPDATED FINAL SAFETY ANALYSIS REPORT

H. B. ROBINSON UNIT 2
TYPICAL FUEL ASSEMBLY
SHEET 1
FIGURE 4.1.2 - 1

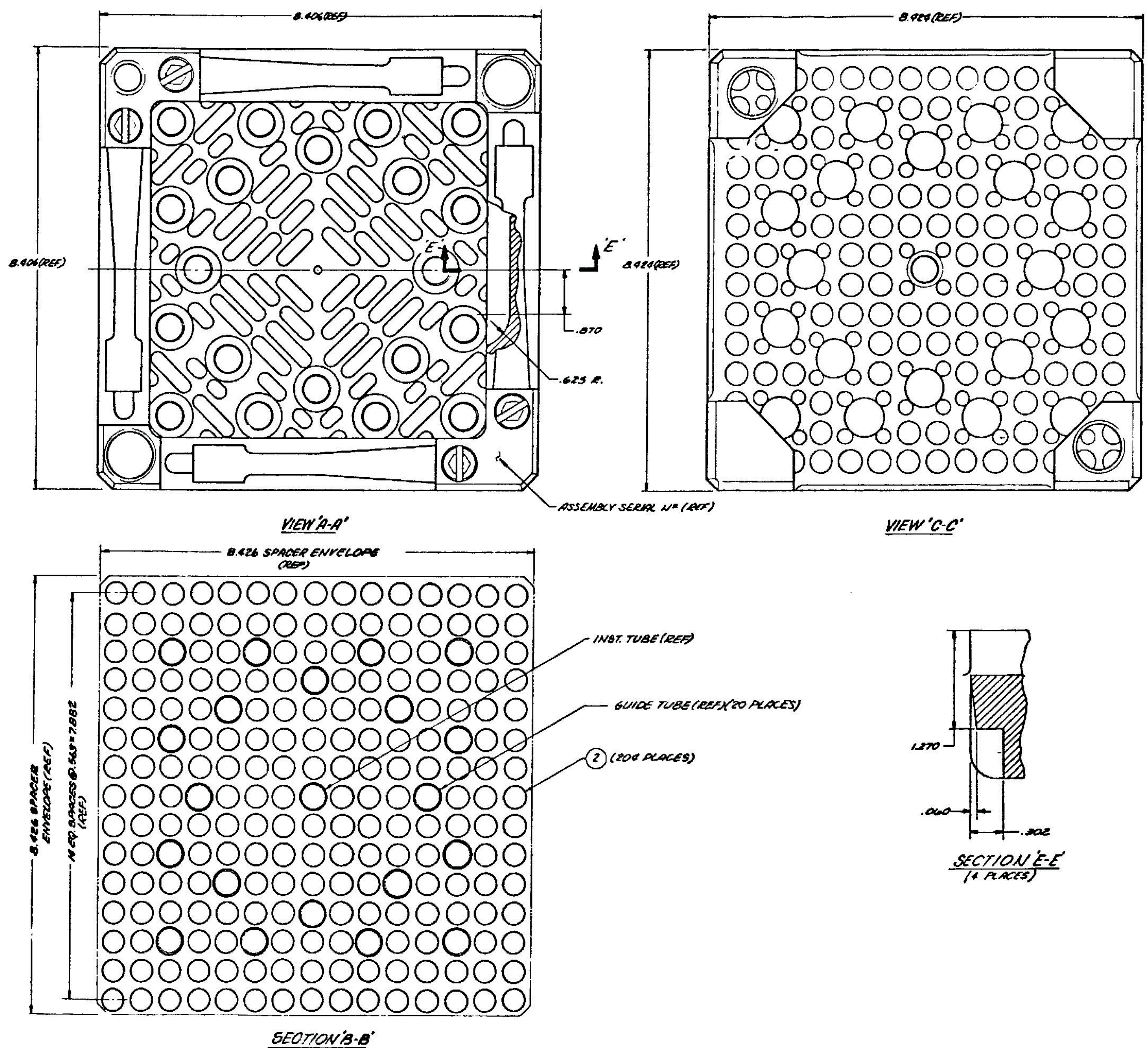

H. B. ROBINSON
UNIT 2
Carolina Power & Light Company
UPDATED FINAL SAFETY ANALYSIS REPORT

H. B. ROBINSON UNIT 2
TYPICAL FUEL ASSEMBLY
SHEET 2
FIGURE 4.1.2 - 2

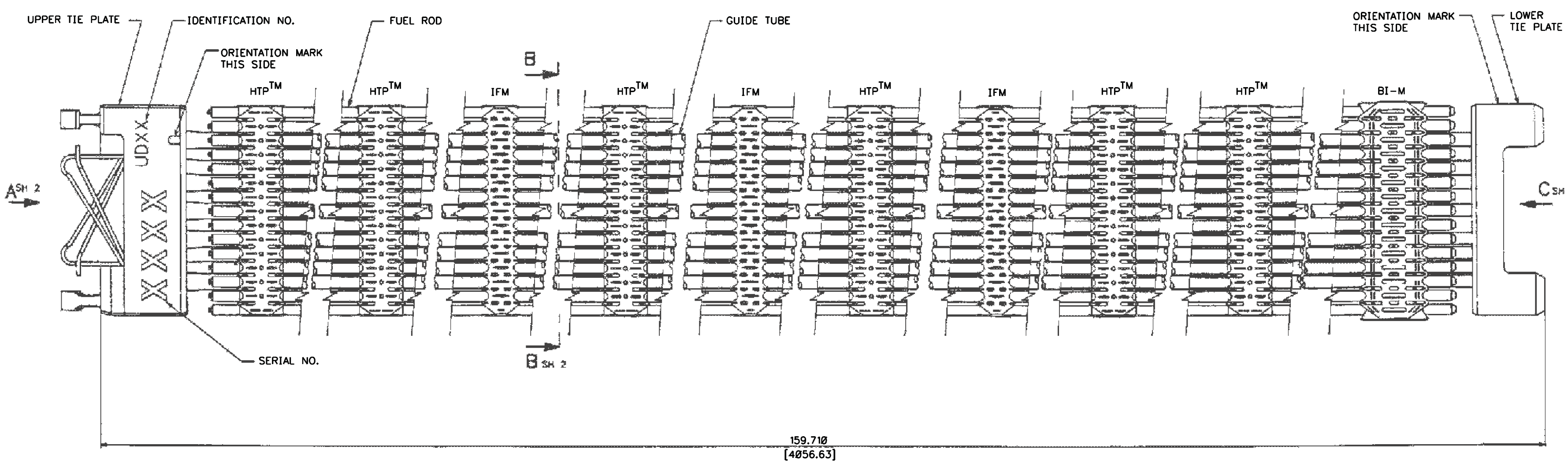

PLAN VIEW

H. B. ROBINSON
UNIT 2
DUKE ENERGY
UPDATED FINAL SAFETY ANALYSIS REPORT

HIGH THERMAL PERFORMANCE™
FUEL ASSEMBLY
SHEET 1

FIGURE 4.1.2-3 REVISION 26

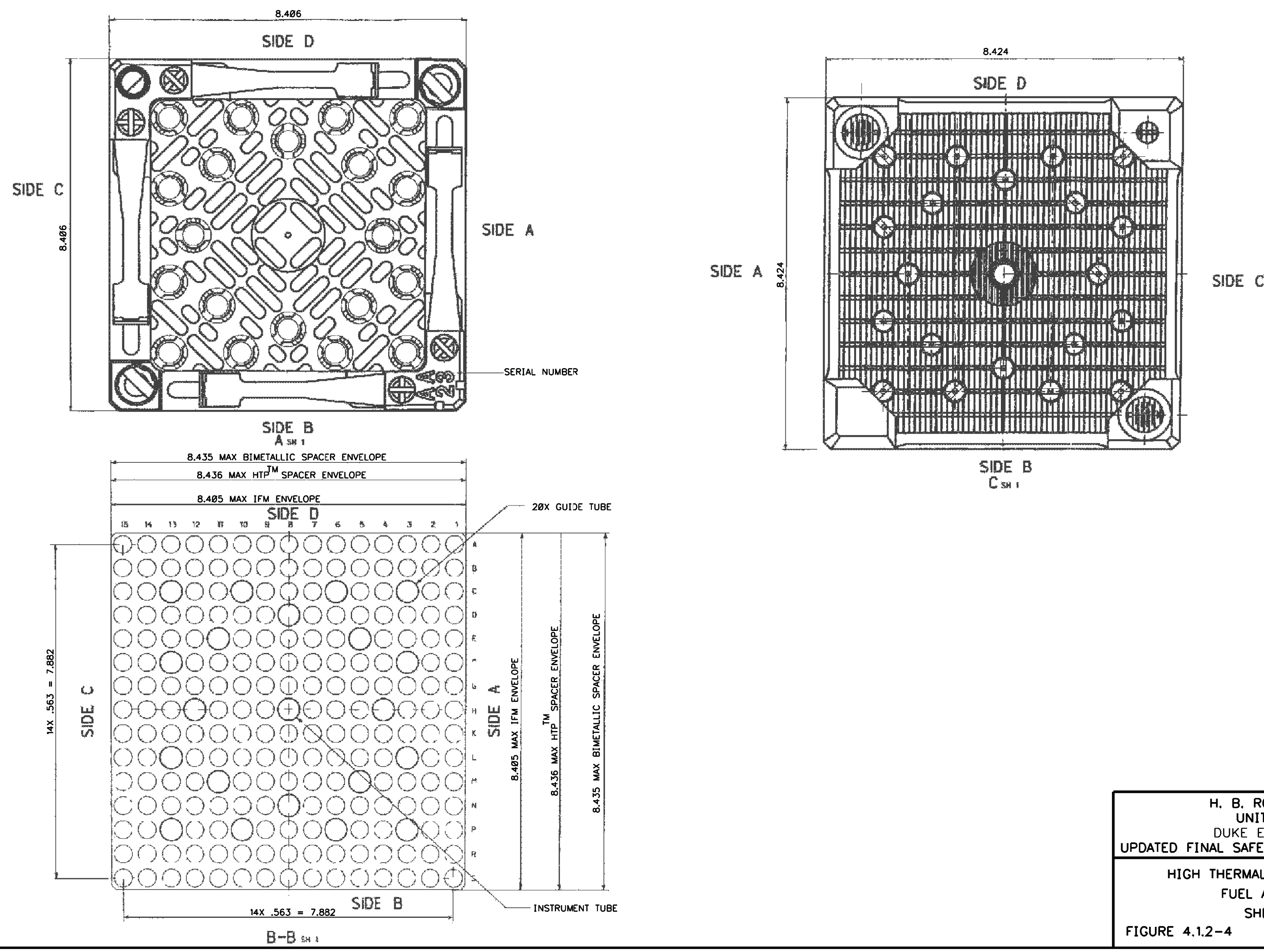

H. B. ROBINSON
UNIT 2
DUKE ENERGY
UPDATED FINAL SAFETY ANALYSIS REPORT

HIGH THERMAL PERFORMANCE™
FUEL ASSEMBLY
SHEET 2

FIGURE 4.1.2-4 REVISION 26

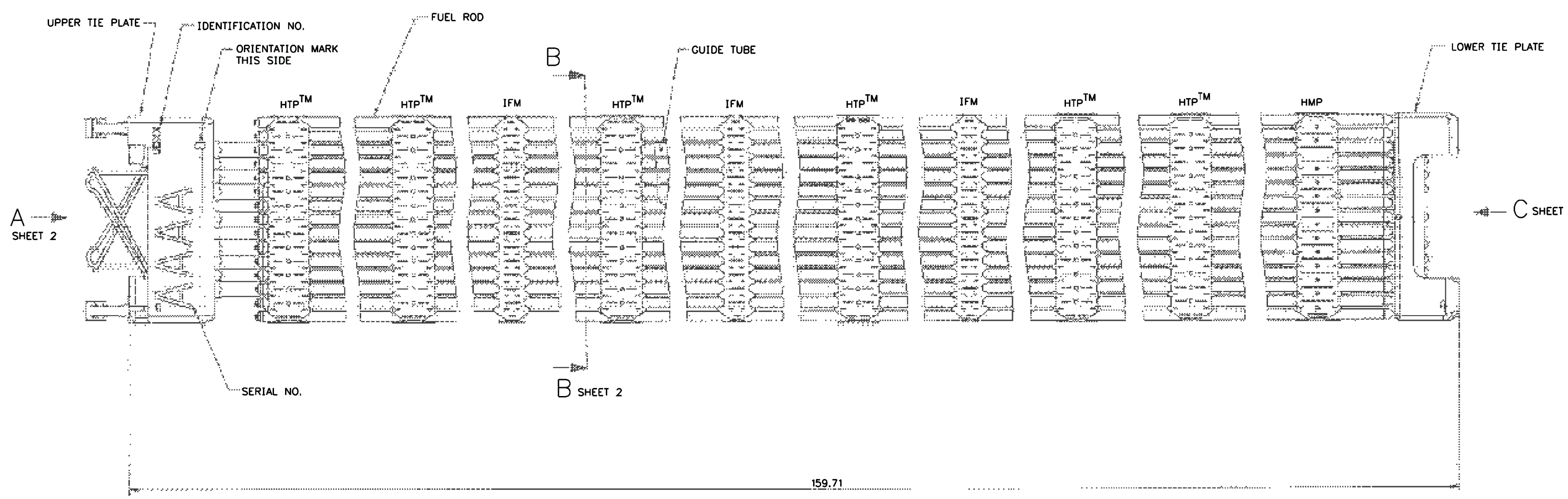

H. B. ROBINSON
UNIT 2
DUKE ENERGY
UPDATED FINAL SAFETY ANALYSIS REPORT

ADVANCED HTP™ FUEL ASSEMBLY
SHEET 1

FIGURE 4.1.2-5

REVISION 26

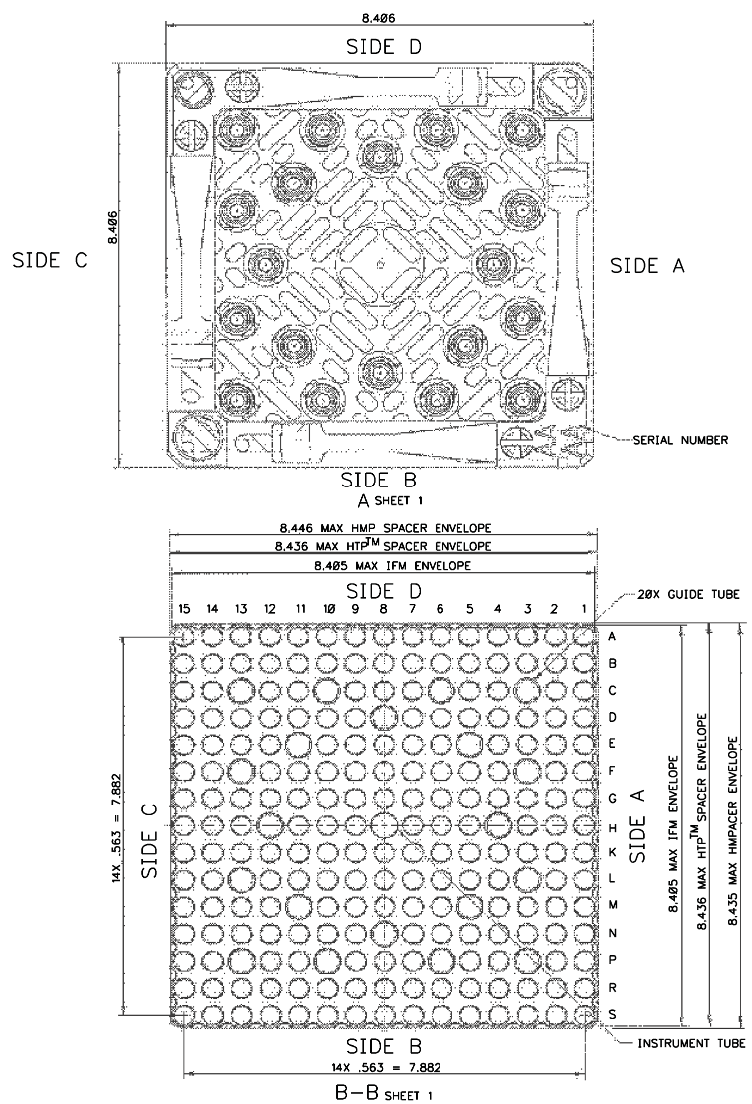

H. B. ROBINSON
UNIT 2
DUKE ENERGY
UPDATED FINAL SAFETY ANALYSIS REPORT

ADVANCED HTP™ FUEL ASSEMBLY

SHEET 2

FIGURE 4.1.2-6

REVISION 26

4.2 Fuel System Design

4.2.1 Design Bases

4.2.1.1 Summary

The fuel design for the H. B. Robinson plant has been modified as follows:

1. Region 17 (ANF-11) incorporated HTP™ and IFM spacers, and a debris resistant lower tie plate. The burnup was increased to 52.5 GWd/MtU peak assembly. Previous axial blanket fuel designs have been analyzed to a peak fuel rod burnup of 53.9 GWd/MtU and a peak fuel assembly burnup of 49.0 GWd/MtU.

2. Region 19 (ROB-13) incorporated the FUELGUARD™ debris resistant lower tie plate design and included part length shielding assemblies (PLSA). The peak fuel rod and peak assembly burnups were reanalyzed to 58.0 GWd/MtU and 54.0 GWd/MtU respectively.

3. Region 20 (ROB-14) incorporated a shorter fuel rod design for higher burnups, and six inch enriched cutback zones between the reduced length (six inch) natural uranium blankets and the central enriched zones of the gadolinia fuel rods. Peak fuel rod burnups were analyzed to 62.0 GWd/MtU, and peak fuel assembly burnups to 57.0 GWd/MtU.

4. Region 27 (ROB-21) incorporated fuel rods using upset shape welding. This process required that the end cap, plenum spring, cladding, and fuel rod assembly be changed. Peak fuel rod burnups were analyzed to 62.0 GWd/MtU and peak fuel assembly burnups to 57.0 GWd/MtU.

5. ROB2-25 (Cycle 25) incorporated pellets with an increased L/D ratio to 1.25 and a new lower end cap with a pedestal. Peak fuel rod burnups were analyzed to 62.0 GWd/MtU and peak fuel assembly burnups to 57.0 GWd/MtU. ROB2-26 had no changes of significance.

6. ROB2-28 (Cycle 28) incorporated 96% theoretically dense pellets with M5® alloy clad and end caps. Peak fuel rod burnups were analyzed to 62.0 GWd/MtU and peak fuel assembly burnups to 58.0 GWd/MtU. Also incorporated HMP™ spacers, MONOBLOC™ guide tubes, and a chamfered pellet.

7. ROB2-31 (Cycle 31) incorporated mid-enriched (2.6%) uranium in the six inch blanket region of the UO_2 fuel pin. The mid-enriched (2.6% Uranium) blanket region of a UO_2-Gd_2O_3 fuel pin is 10.5 inches and the central region is extended to 123 inches. End cap material changed to Zircaloy-4. Peak fuel rod burnups were analyzed to 62.0 GWd/MtU and peak fuel assembly burnups to 58.0 GWd/MtU.

Mechanical design analyses were performed to evaluate cladding steady-state stress and strain, transient strain, fatigue, creep collapse, corrosion, fuel rod internal pressure, elongation, and fuel assembly growth. Design criteria consistent with current AREVA Inc. methodology were used in the analysis. Bounding power histories have been used. The results indicate that all the mechanical design criteria are satisfied.

1. The maximum end-of-life (EOL) steady-state cladding strain was less than the design limit.
2. The cladding strain during power ramps, calculated under different overpower conditions, does not exceed the 1.0 percent strain limit.
3. The cladding fatigue usage factor is within the design limit.

4. The EOL fuel rod internal pressure is less than the approved design limit.
5. The criterion for the prevention of creep collapse is satisfied.
6. The maximum calculated EOL thickness of the oxide corrosion layer is within the design limit.
7. The cladding steady-state stress is within the design limits.

4.2.1.2 Fuel Rod Design Basis

4.2.1.2.1 Cladding physical and mechanical properties

Zircaloy-4 and M5® combine a low neutron absorption cross section, high corrosion resistance, and high strength and ductility at operating temperatures. Principal physical and mechanical properties including irradiation effects on Zircaloy-4 and M5® are provided in Section 4.2.1.2.2 through 4.2.1.2.8.

4.2.1.2.2 Cladding Stress Limits

The design basis for the fuel cladding stress limits is that the fuel system will not be damaged due to fuel cladding stresses exceeding material capability. Conservative limits shown in Table 4.2.1-1 are derived from the ASME Boiler and Pressure Vessel Code, Section III, Article III-2000 (Reference 4.2.1-1) and adapted for M5® cladding (Reference 4.2.4-2).

Normal reactor operation may cause significant pellet cracking and fragmentation. Consequently handling of irradiated fuel assemblies may result in relocation of these fragments against the cladding. Calculations show that high cladding stresses can occur if the reactor power increase is rapid during the subsequent startup. Therefore, the following power ramp rate limits are imposed.

1. During a return to power following a shutdown where fuel assemblies have been handled (e.g., refueling, inspection), the rate of reactor power increase shall be limited to 30 percent of rated power in an hour when below or equal to 50 percent of rated power, 5 percent of rated power in an hour when above 50 percent and below or equal to 90 percent of rated power, and 3 percent of rated power in an hour when above 90 percent of rated power. If during the return to power where fuel assemblies have been handled, the fuel becomes “preconditioned” for a power level as described below, then the “preconditioned” ramp rate maybe used up to that power level.

2. Fuel is considered “preconditioned” up to a specific power level if it has operated at that power level or higher for at least 72 hours. The ramp rate for preconditioned fuel is less than or equal to 30% per hour.

3. Step changes in reactor power should be minimized. The definition of an allowable step change is dependent on the maximum allowable power escalation rate. A “step” is defined as a continuous time period of five minutes or less. Any step change as defined below must be followed by a ten minute hold period (power level held constant for at least ten minutes prior to increasing power). The following step changes are defined along with the ramp rates during which they apply.

   a. 30% FP/hr: >5%FP in < 5 min.
   b. 5% FP/hr: >1.25%FP in < 5 min.
   c. 3% FP/hr: >0.75%FP in < 5 min.

4.2.1.2.3 Cladding Strain Limits

Tests on irradiated tubing (References 4.2.1-2 and 4.2.1-3) indicate potential for failure at relatively low mean strains. The data on tensile, burst and split ring tests, indicate a ductility ranging between 1.2 percent and 5 percent at normal reactor operating temperatures. The failures are usually associated with unstable or localized regions of high deformation after some uniform deformation. To prevent cladding failure due to plastic instability and localization of strain, the total mean hoop cladding strain for steady-state conditions is less than design limits per Reference 4.2.2-2, and the increment of the thermal creep during a transient is limited to 1 percent.

4.2.1.2.4 Strain Fatigue

Cyclic PCI loading combined with other cyclic loading associated with relatively large changes in power can cause cumulative damage which may eventually lead to fatigue failure. Cyclic loading limits are established to prevent fuel failures due to this mechanism. The design life is based on correlations which give a safety factor of 2 on stress amplitude or a safety factor of 20 on the number of cycles whichever is more conservative (Reference 4.2.1-4).

4.2.1.2.5 Fretting Corrosion and Wear

The design basis for fretting corrosion and wear is that fuel rod failures due to fretting shall not occur. Since significant amounts of fretting wear can eventually lead to fuel rod failure, the spacer grid assemblies are designed to prevent such wear.

4.2.1.2.6 Corrosion

Cladding oxidation and corrosion product buildup are limited in order to prevent significant degradation of clad strength. A PWR clad external temperature limit is chosen so that corrosion rates are very slow below this temperature and therefore overall corrosion is limited. An external corrosion layer limit is also specified so that this amount of corrosion will not significantly affect thermal and mechanical design margins. This decrease in clad thickness does not increase clad stresses above allowable levels.

4.2.1.2.7 Hydrogen Absorption

The as-fabricated cladding hydrogen level and the fuel rod cladding hydrogen level during life are limited to prevent adverse effects on the mechanical behavior of the cladding due to hydriding. Hydrogen can be absorbed on either the outside or the inside of the cladding. Excessive absorption of hydrogen can result in premature cladding failure due to reduced ductility and the formation of hydride platelets. Hydrogen absorption is controlled by the oxide layer. Maintaining the oxide layer thickness within the oxide layer limit controls the amount of hydrogen absorption into the zircaloy.

4.2.1.2.8 Creep Collapse

The design basis for creep collapse of the cladding is that significant axial gaps due to fuel densification shall not occur and therefore that fuel failure due to creep collapse shall not occur. Creep collapse of the cladding can increase nuclear peaking, inhibit heat transfer, and cause failure due to localized strain.

If significant gaps form in the pellet column due to fuel densification, the pressure differential between the inside and outside of the cladding can act to increase cladding ovality. Ovality increase by clad creep to the point of plastic instability would result in collapse of the cladding. During power changes, such collapse could result in fuel failure.

Through proper design, the formation of axial gaps and the probability of creep collapse can be significantly reduced. Typical AREVA Inc. pellets are stable dimensionally.

A compressive Inconel plenum spring is included in the fuel rod design and the rods are pressurized with helium to help prevent the formation of gaps in the pellet column.

An analysis is performed in order to guard against the unlikely event that sufficient densification occurs to allow pellet column gaps of sufficient size for clad flattening to occur. The analysis ensures a gap exists between the cladding and the pellet through the densification period of the fuel column.

4.2.1.2.9 Fuel Rod Internal Pressure

The internal gas pressure of the fuel rods may exceed the external coolant pressure up to the NRC approved design limit. Significant outward circumferential creep which may cause an increase in pellet-to-cladding gap must be prevented since it would lead to higher fuel temperature and higher fission gas release.

4.2.1.2.10 Creep Bow

Differential expansion between the fuel rods and lateral thermal and flux gradients can lead to lateral creep bow of the rods in the span between spacer grids. The design basis for fuel rod bowing is that lateral displacement of the fuel rods shall not be of sufficient magnitude to impact thermal margins. The fuel has been designed to minimize creep bow. Extensive post-irradiation examinations have confirmed that such rod bow has not reduced spacing between adjacent rods by more than 50 percent. The potential effect on thermal margins is negligible.

4.2.1.2.11 Overheating of Cladding

The design basis for fuel rod cladding overheating is that transition boiling shall be prevented. Prevention of potential fuel failure from overheating of the cladding is accomplished by minimizing the probability that boiling transition occurs on the peak fuel rods during normal operation and anticipated operational occurrences.

4.2.1.2.12 Overheating of Fuel Pellets

Prevention of fuel failure from overheating of the fuel pellets is accomplished by assuring that the peak linear heat generation rate (LHGR) during normal operation and anticipated operational occurrences does not result in fuel centerline melting. The melting point of the fuel is adjusted for burnup in the centerline temperature analysis.

4.2.1.3 Fuel Assembly Design Bases

4.2.1.3.1 Structural Design

The structural integrity of the fuel assemblies is assured by setting design limits on stresses and deformations due to various handling operational and accident loads. These limits are applied to the design and evaluation of upper and lower tie plates, grid spacers, guide tubes, holddown springs, and locking hardware.

The design bases for evaluating the structural integrity of the fuel assemblies are:

1. Fuel Assembly Handling - Dynamic axial loads approximately 2.5 times assembly weight.

2. For all applied loads for normal operation and anticipated operational events - The fuel assembly component structural design criteria are established for the two primary material categories, austenitic stainless steels (tie plates) and Zircaloy (guide tubes, grids, spacer sleeves). The stress categories and strength theory for austenitic stainless steel presented in the ASME Boiler and Pressure Vessel Code, Section III are used as a general guide.

3. Loads during postulated accidents - Deflections or failure of components shall not interfere with reactor shutdown or emergency cooling of the fuel rods.

4. The fuel assembly structural component stresses under faulted conditions are evaluated using primarily the methods outlined in Appendix F of the ASME Boiler and Pressure Vessel Code, Section III.

4.2.1.3.2 Coolability During Postulated Accidents

The fuel assembly design basis for earthquakes and postulated pipe breaks is that the fuel assembly shall maintain a coolable geometry and control rod insertability during the occurrence of the design seismic/LOCA event.

4.2.1.3.3 Fuel Rod and Assembly Growth

The design basis for fuel rod and assembly growth is that adequate clearance shall be provided to prevent any interference which might lead to buckling or damage. Fuel cladding and guide tube growth measurements are used in establishing the growth correlations used for calculations. Beginning with Reload Region 17 (ANF-11), additional axial fuel rod growth from the higher burnups is provided for with a change in the lower tie plate design that increases the room between the upper and lower tie plates. Reload Region 20 (ROB-14) provides additional growth space for higher burnups through a shorter fuel rod design. Region 27 (ROB-21) increased the overall fuel rod length and was verified for acceptability for shoulder gap.

4.2.1.3.4 Assembly Holddown

The design basis for fuel assembly holddown is that the holddown springs, as compressed by the upper core plate during reactor operation, will provide a net positive downward force during steady-state operation, based on the most adverse combination of component dimensional and material property tolerances. In addition, the holddown springs are designed to accommodate the additional load associated with a pump overspeed transient, and to continue to ensure fuel assembly holddown following such an occurrence.

4.2.1.4 Core Components Design Bases

The reactor internal components are designed to withstand the stresses resulting from startup, steady state operation with any number of pumps running, and shutdown conditions. No damage to the reactor internals occurs as a result of loss of pumping power.

Lateral deflection and torsional rotation of the lower end of the core barrel are limited to prevent excessive movements resulting from seismic disturbances and thus prevent interference with rod cluster control assemblies. Core drop in the event of failure of the normal supports is limited so that the rod cluster control assemblies do not disengage from the fuel assembly guide thimbles.

The structural internals are designed to maintain their functional integrity in the event of a major loss-of-coolant accident (LOCA). The dynamic loading resulting from the pressure oscillations because of a LOCA does not prevent rod cluster control assembly (RCCA) insertion.

The cladding is designed to be free-standing under all operating conditions and will maintain encapsulation of the absorber material throughout the absorber rod design life. Allowance for wear during operation is included in the RCCA cladding thickness.

Adequate clearance is provided between the absorber rods and the guide thimbles which position the rods within the fuel assemblies so that coolant flow along the length of the absorber rods is sufficient to remove the heat generated without oveheating of the absorber cladding. The clearance is also sufficient to compensate for any misalignment between the absorber rods and guide thimbles and to prevent mechanical interference between the rods and guide thimbles under any operating conditions.

TABLE 4.2.1-1

STRESS INTENSITY UNITS

Stress Category	M5® CLADDING STRESS INTENSITY LIMITS Yield Strength	ZIRCALOY-4 CLADDING STRESS INTENSITY LIMITS Yield Strength	Ultimate Tensile Strength
General Primary Membrane	1.0 σ_y (COMP), ⅔ σ_y (TENS)	2/3 σ_y	1/3 σ_u
Primary Membrane Plus Primary Bending	1.0 σ_y	1.0 σ_y	1/2 σ_u
Primary Plus Secondary	2.0 σ_y	2.0 σ_y	1.0 σ_u

4.2.2 Design Description

4.2.2.1 Fuel Assembly

The 15x15 fuel assembly array includes 20 guide tubes, 204 fuel rods and one instrumentation tube. Six of the seven grid spacers are an all-zircaloy High Thermal Performance (HTP™) design. The bottom spacer grid is bi-metallic through ROB2-27 and an Alloy 718 High Mechanical Performance (HMP™) spacer for ROB2-28 and later. There are three Intermediate Flow Mixer (IFM) grids, which along with the HTP™ grids, have internal slanted channels that improve the fuel rod heat transfer and coolant mixing. The fuel assembly tie plates are stainless steel castings with Inconel holddown springs. Beginning with the reload Region 19 (ROB-13), the FUELGUARD™ debris resistant lower tie plate was incorporated into the fuel assembly design. The FUELGUARD™ lower tie plate consists of a curved blade and rod grid brazed into a cast frame. The FUELGUARD™ is designed to prevent coolant entrained debris from passing into the fuel assembly. Fuel assembly characteristics are summarized in Table 4.2.2-1. The bi-metallic and HTP™ fuel assemblies are shown in Figures 4.1.2-1, 4.1.2-3, and 4.1.2-5. Beginning with the reload Region 27 (ROB-21), fuel rod fabrication was changed from TIG to upset shape welding (USW). This process required that the end cap plenum spring, cladding, and fuel rod assembly be changed.

The grid spacers are welded to the Zircaloy-4 guide tubes, and the guide tubes are mechanically attached and secured to the upper and lower tie plates. The instrumentation tube is welded (ROB2-14 through ROB2-27) or mechanically captured by welded rings at the HMP™ spacer (ROB2-28 and later) and is also mechanically captured between tie plates. The fuel rods are axially positioned within the skeleton with approximately equal spacing at both ends except beginning with ROB2-28 where they are biased towards the lower plates. The upper tie plates are designed to be removed and reinstalled by underwater remote handling techniques. Minor changes to the upper tie plates (increasing spring screw engagement) occurred with reload Region 27 (ROB-21).

Proper orientation of fuel assemblies is specifically addressed through the design of the upper tie plate. As shown in Figure 4.1.2-2 and 4.1.2-4, it has two locating holes in opposite corners for receiving the locating pins in the upper core support plate. A third hole of smaller diameter is located in a third corner for the purpose of orienting the assembly. This hole receives the indexing pin from the manipulator grapple.

4.2.2.1.1 Fuel Assembly Material Properties

The material properties used in the design evaluation are described in this section.

4.2.2.1.2 Zircaloy-4 Physical Properties

Zircaloy-4 is used in three forms: (a) cold worked and stress relieved cladding;
(b) recrystallized annealed tubing; and (c) recrystallized annealed strip.

4.2.2.1.3 M5® Physical properties

M5® is used as recrystalized annealed cladding.

4.2.2.1.4 Fissile Material (Uranium Dioxide)

Chemical composition is as follows:

1. Uranium Content - The uranium content shall be a minimum of 87.7 percent by weight of the uranium dioxide on a dry weight basis.

2. Stoichiometry - The oxygen-to-uranium ratio of the sintered fuel pellets shall be within the limits of 1.99 and 2.01.

Mechanical properties are as follows:

1. Mechanistic Fuel Swelling Model - The irradiation environment and fissioning events cause the fuel material to alter its volume and, consequently, its dimensions.

2. Fission Gas Release - For design evaluations of end-of-life pressures, pellet-cladding interaction and general thermal mechanical conditions, a physically based two-stage release model is used. First stage fission gas release is to grain boundaries, and then the second stage release is from the grain boundaries to the interconnected free gas volume.

3. Melting Point - The value used for the UO_2 melting point (unirradiated) is 2790ºC (5054ºF). Based on measurements by Christensen, et al (Reference 4.2.2-1), the melting point is reduced linearly with irradiation at the rate of 12.2ºC (22.0ºF) per 10^{22} fiss/cm^3 or 32ºC (57.6ºF) per 10^4 MWd/MTU.

4.2.2.1.5 Nickel Alloy Springs

Coil springs are fabricated from Nickel Alloy X-750 wire or rod. Leaf springs are fabricated from Nickel Alloy 718 sheet or strip.

4.2.2.2 Fuel Rod

The fuel rods consist of cylindrical UO_2 pellets in Zircaloy-4 (through ROB2-27) or M5® alloy (beginning with ROB2-28) tubular cladding.

The Zircaloy-4 fuel rod cladding is cold worked and stress relieved. M5® alloy fuel cladding is fully annealed. Zirconium alloy plug type end caps are seal welded to each end. The upper end cap has external features to allow remote underwater fuel rod handling. The lower end cap has a truncated cone exterior to aid fuel rod reinsertion into the fuel assembly during inspection and/or reconstitution.

Each non-PLSA fuel rod contains a 132.0 inch column of enriched UO_2 fuel pellets, and a 6 inch column of natural UO_2 fuel pellets at each end except for gadolinia bearing fuel rods which have a 12-inch natural uranium blanket at the top and bottom of the fuel rod. Beginning with reload Region 20 (ROB-14), the gadolinia bearing fuel rods contain a 6-inch natural uranium blanket, and a 6-inch enriched uranium column between the natural blanket and the central gadolinia fuel column at the top and bottom of the fuel rod. Beginning with Region 34 (ROB2-31) the six inch blanket region of a UO_2 fuel pin contains mid-enriched (2.6%) uranium; the mid-enriched (2.6% Uranium) blanket region of a UO_2-Gd_2O_3 fuel pin is 10.5 inches. Each PLSA fuel rod has the bottom 42 inches of fuel replaced by stainless steel.

The fuel rod upper plenum contains an Inconel compression spring to prevent fuel column separation during fabrication and shipping, and during in-core operation.

Fuel rods are pressurized with helium which provides a good heat transfer medium and assists in the prevention of clad creep collapse. The fuel rod is shown in Figure 4.2.2-2.

4.2.2.3 Core Components

4.2.2.3.1 Rod Cluster Control Assembly

The RCCA are provided to control the reactivity of the core under operating conditions. These assemblies, one of which is shown in Figure 4.2.2-3, each consist of a group of individual absorber rods fastened at the top end to a common hub or spider assembly. RCCA details are presented in Table 4.2.2-2.

The absorber material used in the control rods is silver-indium-cadmium alloy which is essentially "black" to thermal neutrons and has sufficient additional resonance absorption to significantly increase its worth. The alloy is in the form of extruded single length rods which are sealed in stainless steel tubes to prevent the rods from coming in direct contact with the coolant.

The overall control rod length is such that when the assembly has been withdrawn through its full travel, the tips of the absorber rods remain engaged in the guide thimbles so that alignment between rods and thimbles is always maintained. Since the rods are long and slender, they are relatively free to conform to any small misalignments with the guide thimble. Prototype tests have shown that the RCCA are very easily inserted and not subject to binding even under conditions of severe misalignment.

The spider assembly is in the form of a center hub with radial vanes containing cylindrical fingers from which the absorber rods are suspended. Handling detents and detents for connection to the drive shaft are machined into the upper end of the hub. A spring pack is assembled into a skirt integral to the bottom of the hub to stop the RCCA and absorb the impact energy at the end of a trip insertion. The radial vanes are joined to the hub and the fingers are joined to the vanes by furnace brazing. A centerpost which holds the spring pack and its retainer is threaded into the hub within the skirt and welded to prevent loosening in service. All components of the spider assembly are made from Type 304 Stainless Steel, except for the springs, which are Inconel X-750 alloy, and the retainer, which is of 17-4 PH material.

The absorber rods are secured to the spider so as to assure trouble free service. The rods are first threaded into the spider fingers and then pinned to maintain joint tightness, after which the pins are welded in place. The end plug below the pin position is designed with a reduced section to permit flexing of the rods to correct for small operating or assembly misalignments.

In construction, the silver-indium-cadmium rods are inserted into coldworked stainless steel tubing which is then sealed at the bottom and the top by welded end plugs. Sufficient diametral and end clearances are provided to accommodate relative thermal expansions and to limit the internal pressure to acceptable levels.

The bottom plugs are made bullet-nosed to reduce the hydraulic drag during a reactor trip and to guide smoothly into the dashpot section of the fuel assembly guide thimbles. The upper plug is threaded for assembly to the spider and has a reduced end section to make the joint more flexible.

Stainless steel clad silver-indium-cadmium alloy absorber rods are resistant to radiation and thermal damage thereby ensuring their effectiveness under all operating conditions.

4.2.2.3.2 Neutron Source Assembly

The H. B. Robinson core normally utilizes one to two neutron source assemblies. Historically, these sources have been composed of four secondary source rods, however, beginning in Cycle 14 source assemblies with eight secondary source rods will be used to increase source strength (this does not preclude a return to sources with four secondary rods in the future). The increased source strength is necessary to overcome the shielding effect of the PLSA assemblies which are located between the sources and the source range detectors. The rods in the secondary source assemblies (both 4 and 8 finger) are fastened to a spider-hub at the top similar to a rod cluster control assembly (RCCA) spiders. In the core, the neutron sources assemblies are inserted into fuel assembly guide tubes at locations that are unrodded and with which there will be mechanical compatibility between the spider-hub and the reactor upper internals. Figure 4.3.2-1 illustrates the preferred secondary source locations of H-03 and H-13.

Beginning in Cycle 20, the neutron sources were removed from the operating core. It was determined that adequate counts could be established using irradiated fuel versus the neutron source bearing assemblies. This, however, does not preclude operation with neutron sources in the future.

General design criteria similar to that for the fuel rods are used for the design of the source rods; i.e., the cladding is free-standing, internal pressures are always less than reactor operating pressure, and internal gaps and clearances are provided to allow for differential expansions between the source material and cladding. Typically, secondary source rods used at H. B. Robinson have utilized cold-worked Type 304 Stainless Steel cladding material (nominal 0.431 in. OD, 0.3935 in. ID) with Sb-Be source pellets of stack height 67.87 in. Alternative designs are possible provided they meet the general design criteria.

In some cases more than two source assemblies may be used in the core to provide an active source during startup while transitioning from old previously irradiated sources to new inactive sources; at the completion of a "source transition cycle" the old sources are typically removed and disposed of. In this circumstance, some source assemblies must be located in core locations other than the preferred locations H-03 and H-13. The following alternative core locations provide mechanical compatibility between the reactor upper internals and the spider-hub type source assemblies utilized at H. B. Robinson:

A-07	A-09	B-07	B-09	B-11	C-04	C-05	C-06
C-10	C-11	D-07	D-09	D-11	D-13	E-02	E-03
E-06	E-13	F-07	G-04	G-10	G-12	G-14	H-01
H-03	H-07	H-13	J-01	J-04	J-06	J-08	J-14
J-15	K-07	K-09	K-13	L-02	L-03	L-04	L-10
L-13	M-05	M-07	M-13	N-05	N-11	N-12	P-05
P-09	P-11	R-08	R-09				

If the purpose of a given source located in a core position other than H-03 or H-13 is to provide counts for the source range detectors, acceptable (but not necessarily exclusive) alternative locations taken from the mechanically compatible list are:

G-04	G-12	G-14	J-04	J-14

In locating a new inactive source for irradiation and use in the following cycle, an additional consideration in choosing its location is that the host assembly should experience a relative power of at least 0.5 to provide sufficient activation.

4.2.2.3.3 Thimble Plug Assembly

In order to limit bypass flow through the RCC guide thimbles in fuel assemblies which do not contain either control rods or source assemblies, the fuel assemblies at those locations are fitted with plugging devices. The plugging devices consist of a flat plate with short rods suspended from the bottom surface and a spring pack assembly attached to the top surface. At installation in the core, the plugging devices fit into the fuel assembly top nozzles and rest on the adaptor plate. The short rods project into the upper ends of the thimble tubes to reduce the bypass flow area. The spring pack is compressed by the upper core when the upper internals package is lowered into place. Similar short rods are also used on the source assemblies to fill the ends of all vacant fuel assembly guide thimbles.

All components in the plugging device, except for the springs, are constructed from Type 304 Stainless Steel. The springs are wound from an age hardenable nickel-base alloy. Beginning with cycle 21, the plugging devices were removed. As a result, the total core bypass flow increased.

TABLE 4.2.2-1 (page 1 of 3)

FUEL ASSEMBLY DESIGN

FUEL PELLET	
Fuel Material	UO_2 Sintered Pellets
Pellet Diameter, (in.)	0.3570
CLADDING	
Clad Material (through ROB2-27/ROB2-28 and later)	Zircaloy-4 Cold Worked and Stress Relieved/M5® alloy fully annealed
Clad ID, (in.)	0.364
Clad OD, (in.)	0.424
Clad Thickness, Nominal, (in.)	0.030
FUEL ROD	
Diameter Gap, Cold Nominal, (in.)	0.0070
Active Length, (in.)	144.0
Total Rod Length, (in.) Through Region 19 (ROB-13)/Region 20 (ROB-14) thru Region 26 (ROB-20)/ Region 27 (ROB-21) to ROB2-25/ ROB2-26 to present	152.065/151.950/151.978/ 151.98
Fill Gas	Helium
BI-METALLIC SPACER (through ROB2-27)	
Number per assembly	1
Material	Zr-4 & Inconel 718
Maximum Envelope (in.)	8.435 square

TABLE 4.2.2-1 (page 2 of 3)

FUEL ASSEMBLY DESIGN

HIGH THERMAL PERFORMANCE (HTP™) SPACER	
Number per assembly	6
Material	Zircaloy-4
Maximum envelope (in.)	8.436 square
HIGH MECHANICAL PERFORMANCE (HMP™) SPACER (beginning with ROB2-28)	
Number per assembly	1
Material	Inconel Alloy 718
Maximum envelope (in.)	8.446 square
INTERMEDIATE FLOW MIXER (IFM) GRID	
Number per assembly	3
Material	Zircaloy-4
Maximum envelope (in.)	8.405 square
GUIDE TUBE (MONOBLOC™ starting with ROB2-28)	
Material	Zr-4, Fully Annealed
OD/ID Above Dashpot (in.)	0.544/0.511
FUEL ASSEMBLY	
Array	15x15
Rod Pitch	0.563
No. Bi-metallic Spacers: (through ROB2-27)	1
No. Alloy 718 HMP™ Spacers (ROB2-28 and later)	1
No. Zircaloy Spacers:	6
No. IFM Grids:	3
No. Fuel Rods	204
No. Guide Tubes	20
No. Instrumentation Tubes	1

TABLE 4.2.2-1 (page 3 of 3)

FUEL ASSEMBLY DESIGN

TIE PLATES	
Material	Stainless Steel
HOLDDOWN SPRINGS	
Material	Inconel
CAP SCREWS	
Material	Stainless Steel

TABLE 4.2.2-2

CORE MECHANICAL DESIGN PARAMETERS*

Active Portion of the Core	
Equivalent Diameter, in.	119.7
Active Fuel Height, in.	144.0
Length-to-Diameter Ratio	1.2
Total Cross-Section Area, ft^2	78.1
Rod Cluster Control Assemblies	
Neutron Absorber	5% Cd, 15% In, 80% Ag
Cladding Material	Type 304 SS - Cold Worked
Clad Thickness, in.	0.019
Number of Clusters, Full Length	45
Number of Control Rods per Cluster	20
Weight in 60°F Water, pounds	147
Length of Rod Control, in.	158.454 (overall)
	150.954 (insertion length)
Length of Absorber Section, in.	142.00
Core Structure	
Core Barrel, in.	
ID	133.875
OD	137.875
Thermal Shield, in.	
ID	142.625
OD	148.0

*All dimensions are for cold conditions

4.2.3 Mechanical Design Evaluation

4.2.3.1 Reactor Operating Conditions for Design

The fuel assembly design is based on the following reactor operating conditions:

NOTE: The values provided below may bound actual values such that a conservative analysis is generated.

Core Power Level	
Nominal	2339 MWt
Design Basis (18% Thermal Overpower)	2760 MWt
Coolant Operating Pressure (Nominal)	2250 Psia
Coolant Flow Rate (Nominal @ Nominal Power)	
Total	108.0×10^{6} lb/hr
Active Core	101.3×10^{6} lb/hr
Heat Generation Fraction Fuel Rods	97.4 percent
Coolant Inlet Temperature (Nominal)	547.6ºF
Core Average Coolant Temperature	577.0ºF
Number of Assemblies in Core	157 (153.5 active)

The fuel shall be capable of load-follow operation between 50 percent and 100 percent of rated power, and not preclude the transients set forth in the UFSAR.

4.2.3.2 Fuel Rod Evaluation

4.2.3.2.1 Design criteria

1. Cladding steady state stresses shall not exceed the established limits.

2. Maximum cladding strain shall not exceed the design limit per Reference 4.2.2-2 and Reference 4.2.4-2 during steady state or during expected transients. (Maximum hoop stresses are bounded by strain limits. See Reference 4.2.3-7 for analysis of hoop stresses.)

3. The cumulative usage factor for cyclic stresses shall not exceed 0.67 for Zircaloy-4 cladding and 0.9 for M5® cladding.

4. The fuel rod internal pressure at the end of the design life may exceed the system operating pressure up to the NRC approved design limit.

5. Cladding creep collapse shall not occur.

6. The thickness of the corrosion layer shall not exceed design limits.

7. The fuel elongation must be accommodated by the clearance between fuel rods and tie plates.

8. Fuel rod creep bow throughout the design life of the assemblies shall be limited so as to maintain licensing and operational limit restraints.

9. The fuel rod plenum spring shall maintain a positive compression on the fuel column during shipping and during the fuel densification stage.

10. Cladding temperatures shall not exceed the design limits.

11. Pellet temperatures shall not exceed the melting temperature during normal operation and anticipated transients.

4.2.3.2.2 Fuel rod analysis

The fuel rod analysis considers the high burnup design with cycle-specific central column and axial blanket enrichments. The power of the limiting neutron absorbing fuel (NAF) shall be less than the limiting UO2 fuel during operation. The analyses described in this Section were originally detailed and documented in References 4.2.3-1, 4.2.3-2, and 4.2.3-6. The impact of fuel thermal conductivity degradation (TCD) with burnup has been considered and included in the fuel rod analyses consistent with NRC's approval of AREVA's treatment of fuel TCD in Reference 4.2.4-3.

1. Steady State Stresses - The cladding steady-state stresses are highest at beginning-of-life except for a bending stress due to ovality. Since the cladding eventually is supported by the pellets, the ovality bending stress is eliminated as a factor for the end-of-life condition at higher burnup. The cladding stresses are within the established limits.

   The stress analysis is performed at the lower end cap since the maximum temperature gradients occur at this end.

   The mechanical stress is caused by the pressure differential across the rod wall and by the axial load of the pellet stack weight and the plenum spring force. The thermal stress is caused by the temperature gradient between the end cap and the heat generating pellets.

   The ANSYS code, which allows thermal as well as stress analyses, was used to model the subject rod region. The maximum weld stress intensity is well below the design limit.

2. Steady State Strain Analyses - The cladding steady-state strain was evaluated with the RODEX2 code. The code calculates the thermal, mechanical and compositional state of the fuel, and cladding for a given duty history. Conservative input values were used in the strain analysis. Dimension values covering all reloads have been analyzed.

   The criterion per Reference 4.2.2-2 and Reference 4.2.4-2 is satisfied.

3. Ramp Strain Analysis - The clad response ramping power changes is calculated with the RAMPEX code. This code calculates the pellet-cladding interaction during a power ramp. The initial conditions are obtained from RODEX2 output. The RAMPEX code considers the thermal condition of the rod in its flow channel and the mechanical interactions that result from fuel creep, crack healing, and cladding creep at any desired axial section in the rod during the power ramp.

The power histories assumed for this analysis include the maximum exposure rods and high power first cycle, second cycle, third cycle, and fourth cycle histories. The high power cycles were used to evaluate large power swings resulting from fuel shuffling.

The conditions at the end of each cycle obtained with the RODEX2 code are used as input data for the RAMPEX code. The rods under consideration were ramped to the maximum power. The maximum strains due to each ramp were examined.

The maximum strains, including primary and secondary thermal creep, were less than the limit given in Reference 4.2.2-2 and Reference 4.2.4-2.

4. Cladding Fatigue Usage Factor - In addition to the ramp strain analyses, a fatigue usage factor for the cladding was calculated. The calculations were based upon the typical duty cycles. Cladding stress amplitudes for the various power cycles were determined from RAMPEX analyses. RAMPEX analyses were run for each cycle at the plane of maximum contact pressure which resulted in conservatively high stresses for the fatigue analysis. The overall fatigue usage factor is within the limit given in Reference 4.2.2-2 and Reference 4.2.4-2.

5. Internal Pressure - A RODEX2 analysis was performed to evaluate the internal fuel rod pressure throughout the fuel lifetime. To prevent cladding instability, the rod internal pressure cannot exceed the approved design limit or else the cladding may creep away from the pellet, which increases the fuel rod pellet temperatures. Higher fuel temperatures result in increased fission gas release and, therefore, higher internal rod pressures. The results of this analysis show the EOL internal rod pressure does not exceed the NRC approved design limit given in Reference 4.2.2-2 and Reference 4.2.4-2. The fuel rod will, therefore, remain stable throughout the expected power history.

6. Creep Collapse - The collapse calculation is done using the RODEX2 and COLAPX codes to determine the temperature and pressure conditions throughout the fuel rod lifetime, and to determine the clad creepdown. These conditions are used as input for COLAPX. The COLAPX code then predicts the time dependent creep ovality deformations in an infinite length tube subjected to external pressure, internal pressure, and linearly varying temperature gradients through the thickness of the cylinder.

   If significant gaps are not allowed to form, then tube ovality, as predicted by the COLAPX evaluation, cannot occur beyond the point of fuel support.

   In order to guard against the highly unlikely event that enough densification occurs to form pellet column gaps of significant size to allow clad flattening, an evaluation was performed. The cladding ovality increase was calculated with COLAPX, and the creepdown was calculated with RODEX2. The combined creepdown at the cladding minor axis was determined not to exceed the minimum level to allow the fuel column to relocate axially without the formation of axial gaps.

7. Rod Bowing - Fuel rod bow is determined throughout the life of the fuel assembly so that reactor operating thermal limits can be established. These limits include the minimum critical heat flux ratio associated with protection against boiling transition and the maximum fuel rod LHGR associated with protection of metal-water reaction and peak cladding temperature limits for a postulated loss of coolant accident (LOCA).

Rod bow measurements have been used to establish an empirical model for determining rod bow as a function of burnup which is used to calculate thermal limits.

The gap spacing data shows that the bow tends to stabilize at higher burnups. In addition, the fuel at high burnups is not limiting from a thermal margin standpoint due to its lower power.

8. Corrosion Layer Analyses - The thickness of the corrosion layer has been evaluated with the RODEX2 code for the peak discharge fuel rod power history. The oxide thickness is within the design limits given in References 4.2.2-2 and 4.2.4-2.

9. Fuel Rod Growth - Growth data has been correlated to fast fluence. Based on this correlation, with an added uncertainty, the rod growth for the maximum discharge exposure fuel rod was calculated. A minimum end of life (EOL) clearance margin for this growth is available.

10. Cladding Temperature - Prevention of potential fuel failure from overheating of the cladding is also established by minimizing the probability that DNB occurs on limiting fuel rods during normal operation and anticipated operating events.

11. Fuel Pellet Temperature - Prevention of fuel failure from overheating of the fuel pellets is accomplished by insuring that the peak LHGR during normal operation and anticipated transients does not result in calculated centerline melt.

4.2.3.3 Fuel Assembly Evaluation

4.2.3.3.1 Design Criteria

The mechanical design criteria for the fuel assembly are listed below:

1. The fuel assemblies shall be mechanically compatible with the reactor core, fuel handling system, and core components.

2. The upper tie plate shall be removable from the fuel assembly to permit access for removal of fuel rods for replacement or inspection.

3. The fuel assembly shall be designed to withstand operating, handling, and accident loads.

4. The fuel assembly shall support the fuel rod, providing sufficient spring force to minimize flow-induced vibrations and to prevent fretting corrosion at the spacer-fuel rod contact points.

5. The assembly shall be designed to provide clearance for irradiation induced guide tube growth without exceeding the core plate-to-core plate spacing.

4.2.3.3.2 Fuel Assembly Analysis

1. Stresses and Deflections - The guide tubes along with the upper and lower tie plates and grid spacers provide the principal structure for the fuel assembly. Guide tubes are considered as restrained columns and are analyzed accordingly, using appropriate load combinations. Column deflection is permissible within constraints of allowable bending stress, allowable displacement, and allowable approach to column instability. The allowable total stress, primary plus bending, is less than the yield strength of the material at the temperature of the load conditions.

   As the power level of the reactor is increased, differential thermal expansion between the Zircaloy guide tubes and the hotter Zircaloy or M5® clad fuel rod would tend to put the guide tube in tension. Therefore, there is no concern as to the stability of the guide tube on approach to normal operating conditions. After some period at power, vibration loads would tend to reduce or eliminate loads caused by differential thermal expansion. Upon reduction in power, differences in temperature between the guide tubes and fuel rods would decrease causing compression loading on the guide tube. Thus, the stability of Zircaloy guide tubes is of most concern as the power level is reduced.

   The Zircaloy spacer was analyzed using a finite element structures code. The structural integrity was confirmed through strength tests. Some tests used a hydrided spacer in order to simulate in-reactor conditions.

   The most severe normal loading condition is the situation where the lower tie plate becomes hung up on a spacer edge during fuel handling. Both analyses and tests indicate that the spacer structure can take such loading.

   Cyclic loading due to differential thermal expansion between the fuel rods and guide tubes is less severe than the assumed refueling load described above. In this latter case the maximum load is uniformly distributed across the spacer structure as compared to the refueling situation load which is concentrated at local regions at the spacer edge. Thus, loading due to differential thermal expansion of the structure should not result in stresses sufficient to cause fatigue failures.

2. Fuel Rod Support – The Zircaloy-4 and Inconel spacer springs are known to relax during irradiation and the fuel rod cladding tends to creepdown. Together, these two characteristics combine to reduce the spacer spring force on a fuel rod during its lifetime. These characteristics have been considered in the design of the spring to assure an adequate holding force when the assembly has completed its design operating life.

   The prevention of fretting corrosion in the Zircaloy HTP™ and IFM spacers is demonstrated by a combination of analysis and fretting tests. The design analysis determines the projected maximum end-of-life gap, considering spring relaxation, clad creepdown, minimum fuel rod outer diameter, and minimum initial spring deflection. Flow test data are used to confirm that fretting corrosion will not occur for the largest possible projected gaps.

3. Fuel Assembly Growth - The limiting condition for fuel assembly growth is at end-of-life after cooldown. Because of the higher coefficient of thermal expansion for the stainless steel core structure relative to the Zr-4 guide tubes, differential thermal expansion increases the assembly/internals structure clearance during heatup and reduces the clearance upon cooldown. Axial growth data for the fuel designs of interest are given in References 4.2.3-1, 4.2.3-2, and 4.2.3-6. Allowing for measurement error and other uncertainties, the maximum EOL fuel assembly length predicted from the upper limits of the data leaves a clearance with the minimum as-built core plate to core plate separation.

4. Combined Shock and Seismic Loading (Internals) - The results of a detailed study of the blowdown plus seismic excitation of the reactor internal indicated that the maximum deflections and stresses in the critical structures are below the established allowable limits. For the transverse excitation, it was shown that the upper barrel would not buckle during a hot-leg break and that it would have an allowable stress distribution during a cold-leg break. Even though control rod insertion is not required for plant shutdown, the analysis shows that none of the guide tubes will deform beyond the "no loss of function" limits established experimentally for control rod insertion, and 52 out of 53 guide tubes would deform less than the conservatively established allowable limit. Consequently, it is concluded that the reactor internals will be able to withstand the assumed accident conditions without becoming distorted enough to prevent adequate core cooling or reactor shutdown.

5. Combined Shock and Seismic Loading (Fuel Assembly) - The reload fuel was evaluated for combined seismic and loss-of-coolant accident (LOCA) mechanical response (Reference 4.2.3-4). The postulated accident condition considered was a 0.2-g seismic event combined with a 144-square-inch pipe break at the cold leg reactor pressure vessel inlet nozzle.

The lateral core plate motions for the seismic and LOCA events were combined based on maximum fuel assembly loads and displacements. The vertical forces from the pipe break at the cold leg reactor pressure vessel inlet nozzle were determined from a summation of pressure differentials acting across a given element, flow stagnation, orifice losses, and friction losses. In addition to these hydraulic forces, gravity forces, buoyancy forces, and holddown spring preload were also included in the analysis.

The combined seismic-LOCA structural analyses were performed utilizing essentially four primary finite element models.

1. Lateral Core Model,

2. Lateral Fuel Assembly Model,

3. Vertical Internals Model,

4. Vertical Fuel Assembly Model

The basic criteria for acceptability for the postulated faulted condition is to provide high assurance that the reactor core can be brought safely to a cold shutdown condition. To demonstrate acceptability, the response of the spacer grid, guide tube, and fuel rod fuel assembly components were evaluated. The evaluations were based on structural responses derived from the finite element models.

Based on the dynamic analysis for the spacer grid response loads, two evaluations were performed. First, a quantified amount of permanent deformation of the spacer grid was compared to an allowable deformation value which would ensure no more than a 5 percent reduction in DNB margin. The grid permanent deformation was determined by comparison to test data. Second, control rod insertion capability was evaluated based on misalignment of the guide tubes in the deformed grid. A combination of test data and analytical calculations was used to show that insertability was not impaired.

The control rod guide tubes were evaluated for maximum stress intensity and critical buckling load. The guide tube stresses were generated by ratioing test strain data based on the lower nozzle axial impact load and maximum fuel assembly lateral deflection. These stresses and the axial load obtained from these stresses were compared to the design limit stress intensity and a factored Euler critical buckling load.

The fuel rods were evaluated for maximum stress intensity. Operational steady-state fuel rod stresses were determined from a detailed static finite element analysis. As was done for the guide tubes, the fuel load stresses were generated by ratioing test strain data. The final stress intensities were compared to the design limit stress intensity.

From the above evaluations, the overall acceptability of the reload fuel for Westinghouse PWR's subjected to the combined postulated seismic-LOCA event was demonstrated.

4.2.4 Testing and Inspection Plan

4.2.4.1 Quality Assurance Program

Information on the DEP Quality Assurance Program is provided in Chapter 17 of the updated FSAR. The AREVA Quality Management Manual for the Fuel Sector is described in Reference 4.2.4-1.

4.2.4.2 Quality Control

Fuel assembly quality control is achieved by a component inspection program which has the following features:

1. An enrichment verification program which covers incoming UF_6 gas to completed fuel rods

2. Verification of cladding integrity by testing and inspection of each lot of tubing received

3. Inspection of fuel pellets for conformity to specification

4. Radiographic examinations

5. Inspection of each fuel assembly for cleanliness, straightness, envelope, rod-to-rod spacing, length and fuel rod axial position, and

6. On-site visual inspection of each fuel assembly based on the condition of the shipping containers including the accelerometers.

REFERENCES: SECTION 4.2

4.2.1-1 ASME Boiler and Pressure Vessel Code, Section III, 1971 Edition, ASME, New York, NY.

4.2.1-2 A. A. Bauer, L. M. Lowry, and J. S. Perrin, Process on Evaluating Strength and Ductility of Irradiated Zircaloy During July through September 1975. BMI-1938, September 1975.

4.2.1-3 A. A. Bauer, L. M. Lowry, W. J. Gallaugher, and A. J. Markworth, Evaluating Strength and Ductility of Irradiated Zircaloy - Quarterly Progress Report January through March 1978, NUREG/CR-0085, BMI-2000, June 1978.

4.2.1-4 W. J. O'Donnel and B. F. Langer, "Fatigue Design Bases for Zircaloy Components," Nuclear Science and Engineering, Volume 20, January 1964.

4.2.2-1 J. A. Christensen, et al, "Melting Point of Irradiated UO_2," WCAP-6065, February 1965.

4.2.2-2 EMF-92-116(P)(A), Revision 0, "Generic Mechanical Design Criteria for PWR Fuel Designs," Siemens Power Corporation, February 1999.

4.2.3-1 ANF-89-164(P), "Mechanical Licensing Report for H. B. Robinson High Thermal Performance Assemblies," November 1989.

4.2.3-2 XN-NF-87-17(P), "Mechanical Design Report For H. B. Robinson Extended Burnup Fuel Assemblies," March 1987.

4.2.3-3 Deleted by Amendment No. 12

4.2.3-4 XN-NF-76-47 (P)(A), "Combined Seismic-LOCA Mechanical Evaluation for Exxon Nuclear 15x15 Reload Fuel for Westinghouse PWR's," November 1981.

4.2.3-5 Deleted

4.2.3-6 ANF-91-149(P), "H. B. Robinson High Burnup Mechanical Licensing Report for ANF-12 and Beyond," August 1991.

4.2.3-7 EMF-94-223(P), "H. B. Robinson High Burnup Mechanical Licensing Report for Reload ROB-14," December 1994.

4.2.4-1 FMM, Revision 2, "Fuel Business Unit Management Manual", May 2011.

4.2.4-2 BAW-10240 (P)(A), Revision 0, "Incorporation of M5™ Properties in Framatome ANP Approved Methods ", Framatome ANP, May 2004.

4.2.4-3 EMF-92-116(P)(A), Revision 0, Supplement 1(P)(A), Revision 0, “Generic Mechanical Design Criteria for PWR Fuel Designs”, AREVA Inc., February 2015.

Figure 4.2.2-1
was deleted by Revision No. 13

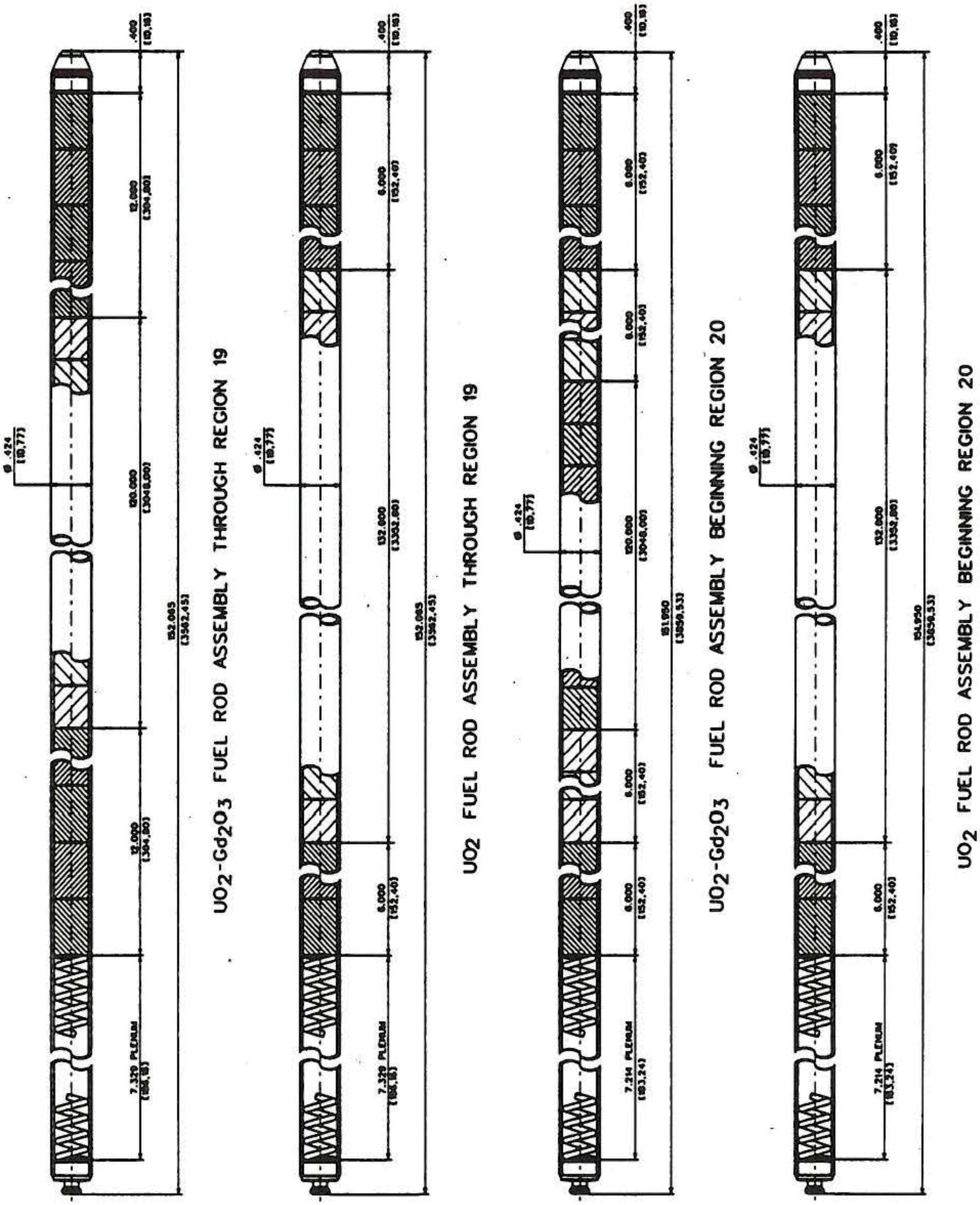

REVISION NO. 13

H. B. ROBINSON UNIT 2 Carolina Power & Light Company UPDATED FINAL SAFETY ANALYSIS REPORT	Fuel Rod Assembly	FIGURE 4.2.2-2

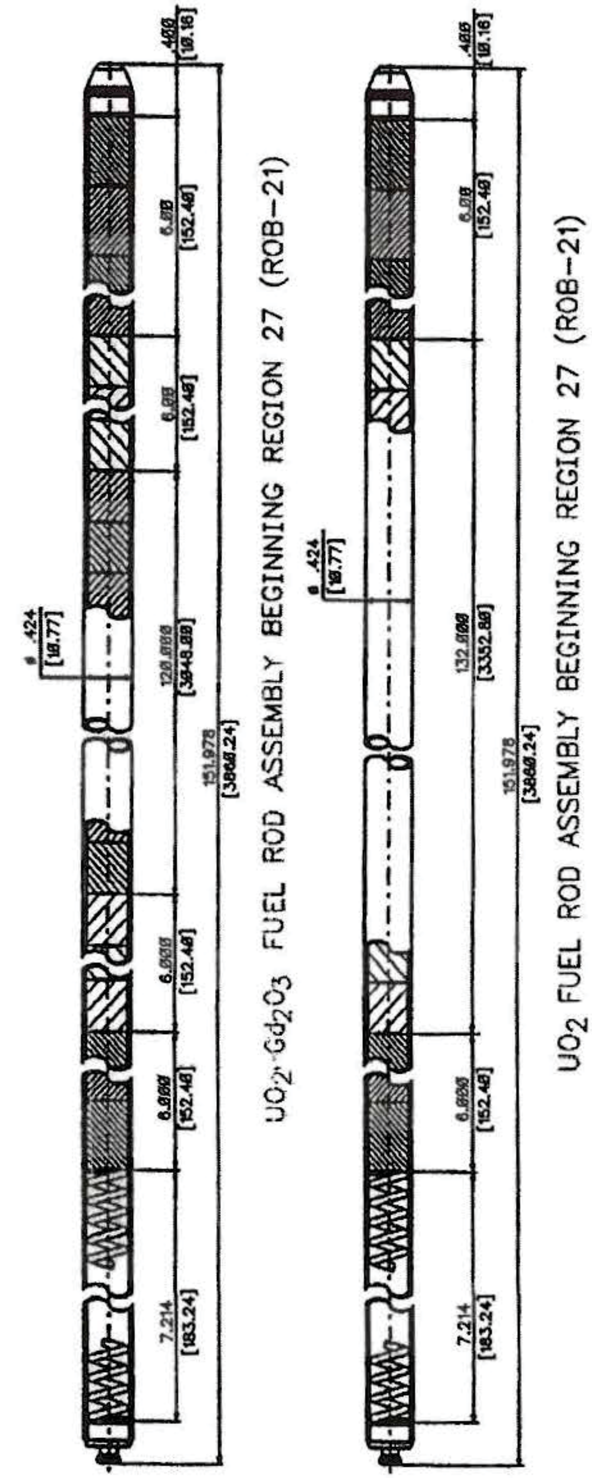

REVISION NO. 20

H.B. ROBINSON UNIT 2 Carolina Power & Light Company UPDATED FINAL SAFETY ANALYSIS REPORT	Fuel Rod Assembly	FIGURE 4.2.2.-2A

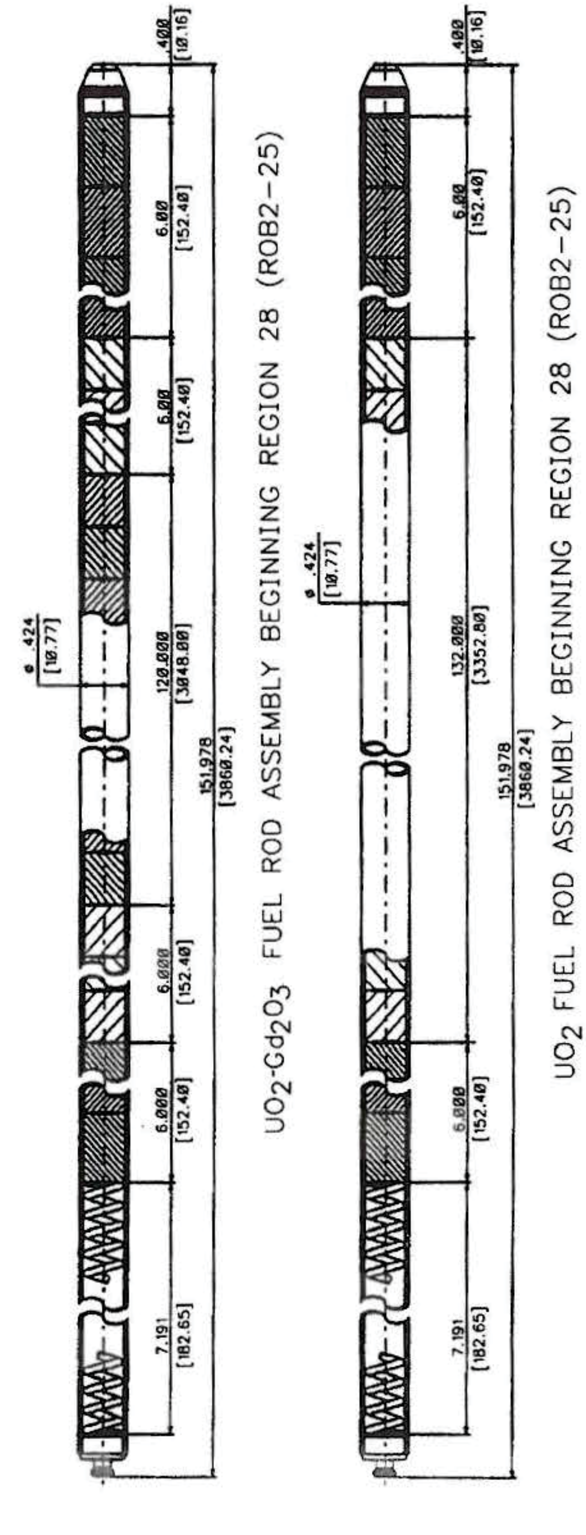

REVISION NO. 21

H.B. ROBINSON UNIT 2 Carolina Power & Light Company UPDATED FINAL SAFETY ANALYSIS REPORT	Fuel Rod Assembly	FIGURE 4.2.2.-2B

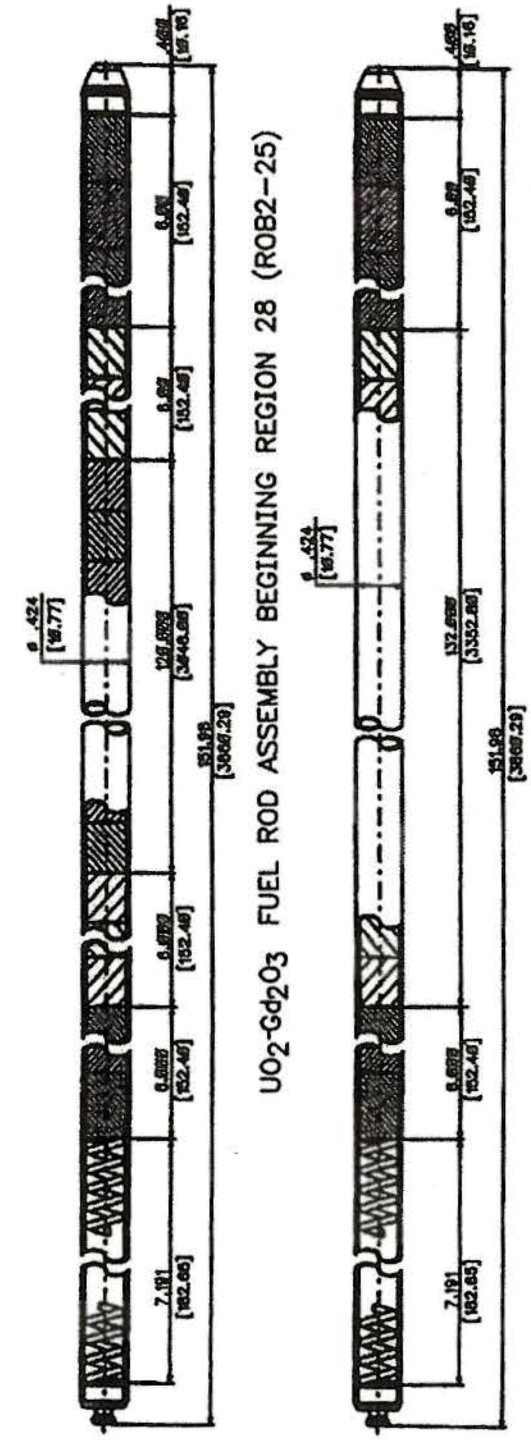

UO_2-Gd_2O_3 FUEL ROD ASSEMBLY BEGINNING REGION 28 (ROB2-25)

UO_2 FUEL ROD ASSEMBLY BEGINNING REGION 28 (ROB2-25)

REVISION NO. 22

H.B. ROBINSON UNIT 2 Carolina Power & Light Company UPDATED FINAL SAFETY ANALYSIS REPORT	Fuel Rod Assembly	FIGURE 4.2.2.-2C

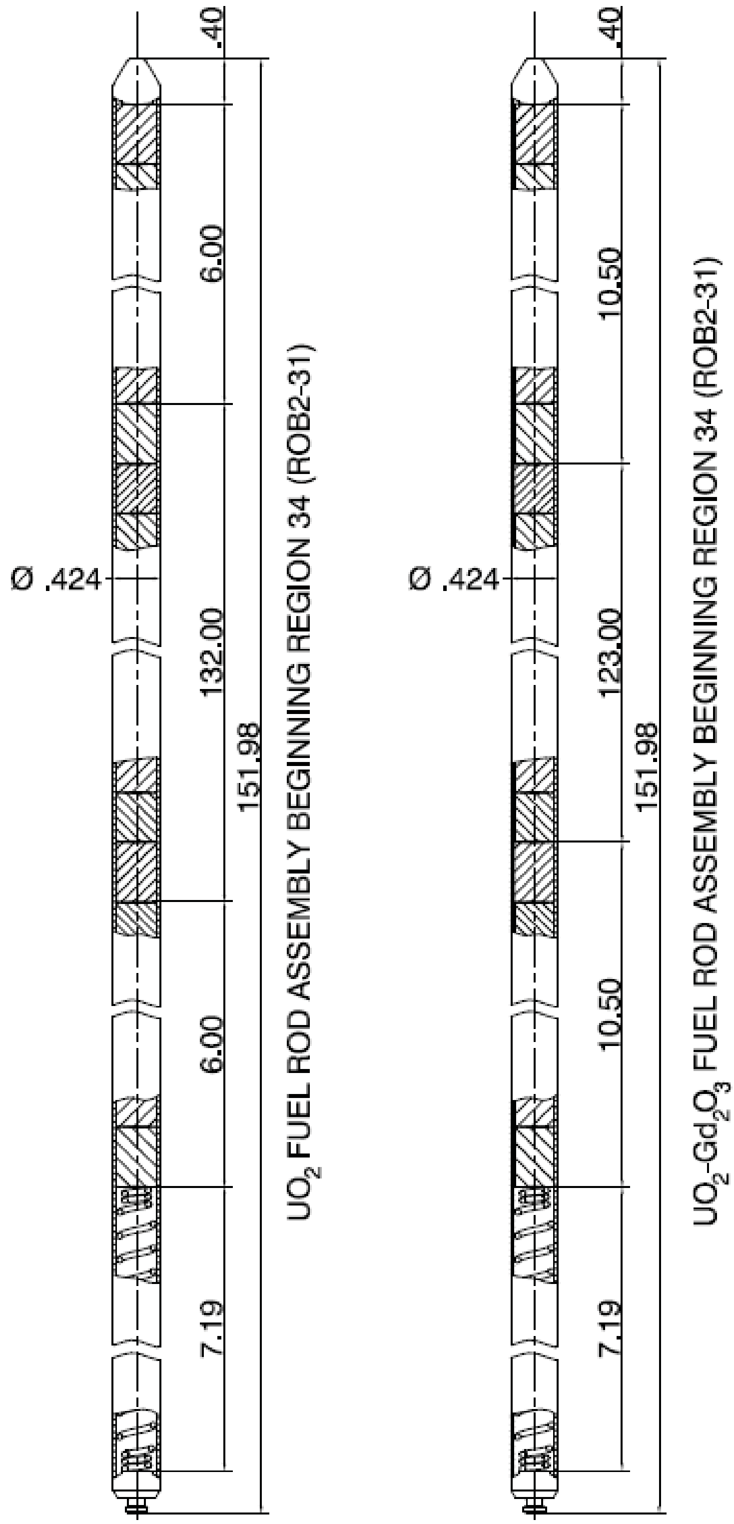

Revision No. 27

H. B. Robinson Unit 2 Duke Energy UPDATED FINAL SAFETY ANALYSIS REPORT	Fuel Rod Assembly	FIGURE 4.2.2-2D

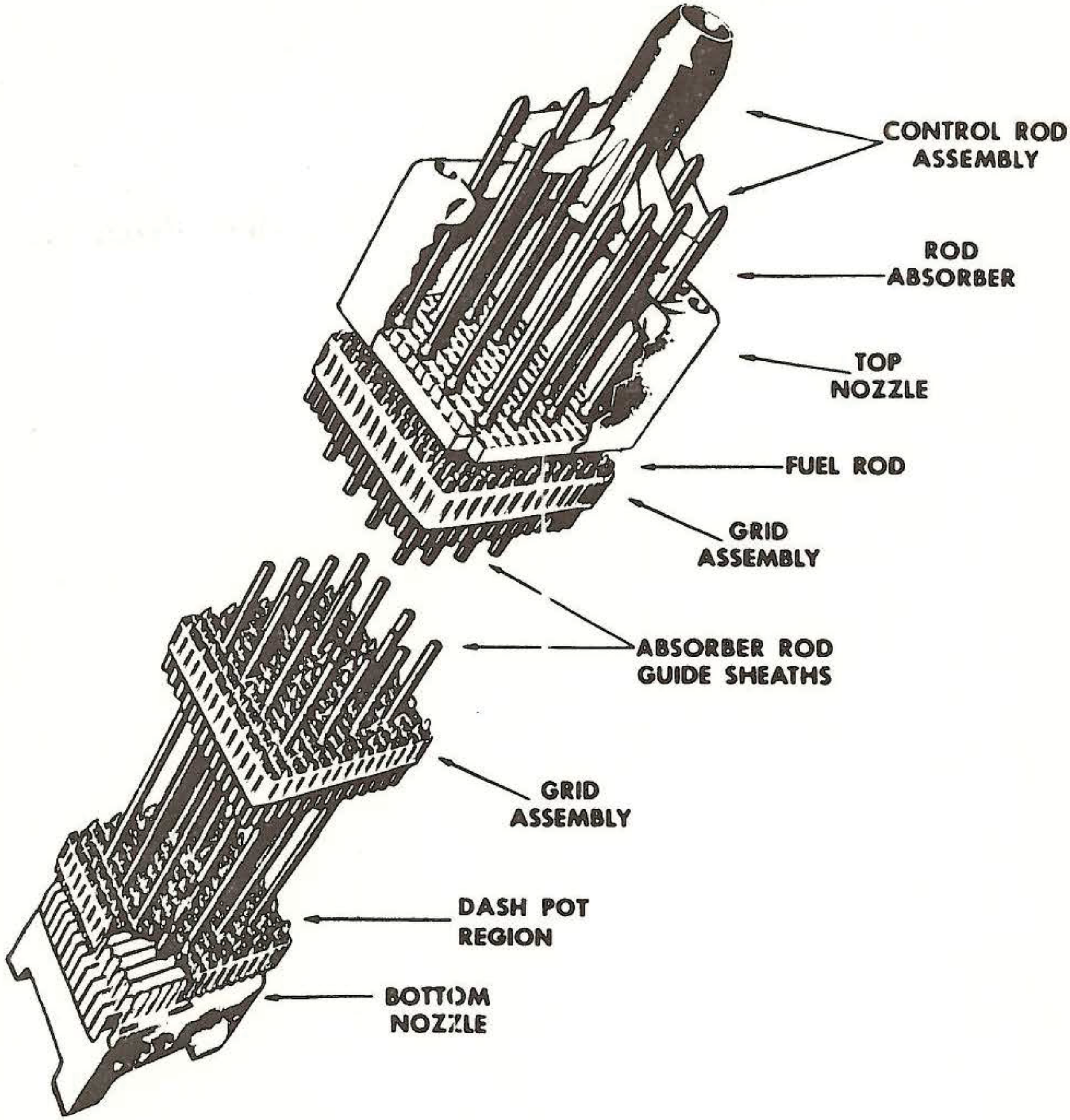

AMENDMENT 3

H. B. ROBINSON UNIT 2 Carolina Power & Light Company UPDATED FINAL SAFETY ANALYSIS REPORT	ROD CLUSTER CONTROL ASSEMBLY	FIGURE 4.2.2 - 3

4.3 Nuclear Design

4.3.1 Design Basis

Nuclear design bases have been established to assure that the reactor core is operated within the HBR 2 Technical Specifications, Appendix A to Facility Operating License No. DPR-23.

4.3.1.1 Fuel Burnup

Fuel burnup is restricted by a limit on peak assembly burnup of 57,000 MWd/MTU for Region 20 (ROB-14) through ROB2-27. For ROB2-28 and later, the peak assembly burnup is limited to 58,000 MWd/MTU. Additionally, PLSA's are explicitly analyzed for compliance to the criteria in Section 4.2.1, with consideration given on a case-by-case basis for residence time extensions (typically six 18-month cycles).

These restrictions represent the burnup and residence time limits for the mechanical evaluation only. Utilization of the full extent of this mechanical burnup limit is contingent on the burnup limit established in the radiological assessments of Chapter 15.

4.3.1.2 Negative Reactivity Feedbacks (Reactivity Coefficients)

The initial core and all reload cores are not allowed to have a positive moderator temperature coefficient when operating above 50% power.

4.3.1.3 Control of Power Distributions

The full loading pattern shall achieve power distributions such that the peak F_Q (including uncertainties) shall not exceed the limit in the Technical Specification in any single fuel rod throughout the cycle under nominal full power operations.

4.3.1.4 Maximum Controlled Reactivity Insertion Rate

The maximum reactivity worth of control rods and the maximum rates of reactivity insertion employing control rods are limited so as to preclude rupture of the reactor coolant pressure boundary or disruption of the core internals to a degree which would impair core cooling capacity due to a rod withdrawal or a rod ejection accident.

4.3.1.5 Shutdown Margins

The fuel loading pattern shall achieve control rod reactivity worths such that the scram worth of all rods minus the most reactive rod shall exceed the beginning of cycle (BOC) and end of cycle (EOC) shutdown requirements.

4.3.1.6 Stability

The protection system ensures that the nuclear core limits are not exceeded during the course of axial xenon oscillations.

4.3.1.7 Emergency Shutdown Capability

Redundant equipment is provided to add soluble poison to the reactor coolant in the form of boric acid to maintain shutdown margin when the reactor is cooled to ambient temperatures.

4.3.2 Description

4.3.2.1 Nuclear Design Description

The HBR 2 reactor core consists of 157 assemblies, each having a 15 x 15 fuel rod array. Each assembly normally contains 204 fuel rods, 20 rod cluster control (RCC) guide tubes, and one instrumentation tube. The fuel rods consist of slightly enriched (in U-235) UO_2 or UO_2 - Gd_2O_3 pellets inserted into Zirconium alloy tubes. The uranium enrichment in the gadolinia pins varies roughly inversely with the gadolinia concentration. The RCC guide tubes and the instrumentation tube are also Zircaloy tubes. Each AREVA Inc. assembly contains 6 Zircaloy spacers and 1 bottom spacer with Inconel 718 springs. Six of the spacers are located within the active fuel region. Prior to ROB2-28, the bottom spacer was bimetallic. For ROB2-28 and later, the bottom spacer is an HMP™. There are also three Intermediate Flow Mixer (IFM) grids.

The average enrichment for each AREVA Inc. reload is consistent with the specified reactor energy requirement for the projected effective full power days for that cycle and subsequent cycles. A loading pattern for each cycle is identified which satisfies the criteria on the peak $F_{\Delta H}$ and the largest calculated axial peaking factor. The fuel centerline melt criterion for the UO_2 rods is set to ensure that the gadolinia pins are never the limiting pins in the assembly, even taking into account the reduced thermal conductivity and melting point in these pins due to the gadolinia. For each specified cycle length the calculated end of cycle critical boron concentration is determined.

The excess reactivity control characteristics are determined for each cycle. These include the differential boron worth at full power conditions as a function of cycle lifetime and control rod worths, including the stuck and ejected rod worths. Control rod shutdown margins and reactivity coefficients are also determined for each fuel cycle.

The effective delayed neutron fractions at BOC and EOC are also calculated for each fuel cycle.

Table 4.1.2-3 presents a summary of some key neutronic characteristics for a typical core loading.

4.3.2.2 Power Distributions

Power distribution control is necessitated by reactor safety considerations. The reactor must be capable of safe operation throughout core life, under both steady state and transient conditions, without exceeding acceptable fuel damage limits. If this performance objective is met, the release of unacceptable amounts of fission products to the reactor coolant is prevented.

To this end, two criteria have been chosen as a design basis for fuel performance related to fission gas release, pellet temperature, and cladding mechanical properties. First, the peak value of linear power density must not exceed the applicable cycle-specific fuel centerline melt criterion (Chapter 15). Second, the minimum departure from nucleate boiling ratio (DNBR) in the core must not be less than the safety limit in normal operation or in short-term transients.

In addition to the above design basis for fuel performance, the initial steady state conditions for the peak linear power for a loss-of-coolant accident (LOCA) must not exceed the values assumed in the accident evaluation (Chapter 15.0). This limit is required in order for the maximum clad temperature attained during a postulated LOCA to remain below that established by the Emergency Core Cooling System (ECCS) Acceptance Criteria.

To aid in specifying the limits on power distribution the following hot channel factors are defined:

1. F_Q, Heat Flux Hot Channel Factor, is defined as the maximum local heat flux on the surface of a fuel rod divided by the average fuel rod heat flux, allowing for manufacturing tolerances on fuel pellets and rods.

2. F_Q^N, Nuclear Heat Flux Hot Channel Factor, is defined as the maximum local fuel rod linear power density divided by the average fuel rod linear power density, assuming nominal fuel pellet and rod dimensions.

3. F_Q^E, Engineering Heat Flux Hot Channel Factor, is defined as the allowance on heat flux required for manufacturing tolerances. The engineering factor allows for local variations in enrichment, pellet density and diameter, surface area of the fuel rod and eccentricity of the gap between pellet and clad. Combined statistically the net effect is a factor of 1.03 to be applied to fuel rod surface heat flux.

4. $F_{\Delta H}^N$, Nuclear Enthalpy Rise Hot Channel Factor, is defined as the ratio of the integral of linear power along the rod with the highest integrated power to the average rod power.

It should be noted that $F_{\Delta H}^N$ is based on an integral and is used as such in the DNB calculations. Local heat fluxes are obtained by using hot channel and adjacent channel explicit power shapes which take into account variations in horizontal (x-y) power shapes through the core. Thus, the horizontal power shape at the point of maximum heat flux is not necessarily directly related to $F_{\Delta H}^N$.

It has been determined by extensive analysis of possible operating power shapes that the design limits on peak local power density and on minimum DNBR at full power are met, provided the values of F_Q and $F_{\Delta H}$ specified in the HBR 2 Technical Specifications are not exceeded.

In accordance with core reload design procedures, there is a required design margin that ensures flux maps performed during operation do not challenge the F_Q Technical Specification limits. During a measurement taken with the movable incore detector flux mapping system, experimental and manufacturing uncertainties must also be accounted for. The appropriate multiplier for this is 1.0815.

In accordance with core reload design procedures, there is a required design margin that ensures flux maps performed during operation do not challenge the $F_{\Delta H}$ Technical Specification limits. During a measurement taken with the movable incore detector flux mapping system, measurement uncertainty must also be accounted for. The appropriate multiplier for this is 1.04, which means that the normal operation of the core will result in a measured $F_{\Delta H}^N$ at least 4 percent less than the value at rated power. The logic behind the larger design uncertainty in this case is that (a) abnormal perturbation in the radial power shape (e.g., rod misalignment) affects $F_{\Delta H}^N$ in most cases without necessarily affecting F_Q^N, and can limit it to the desired value; (b) while the operator has some control over F_Q^N, through F_z^N by motion of control rods, the operator has no direct control over $F_{\Delta H}^N$, and (c) an error in the predictions for radial power shape which may be detected during startup physics tests can be compensated for in F_Q^N by tighter axial control, but compensation for $F_{\Delta H}^N$ is less readily available.

An upper bound envelope of peaking factors has been determined from extensive analysis considering all operating maneuvers consistent with the HBR 2 Technical Specifications on power distribution control. The specifications on power distribution control ensure that xenon distributions are not developed which, at a later time could cause greater local power peaking even though the flux difference is then within limits. The results of an analysis of a postulated LOCA analysis based on this upper bound envelope indicate that the peak clad temperature would not exceed the 2200°F limit set forth in the ECCS Acceptance Criteria. The nuclear analyses of possible credible power shapes consistent with the power distribution control procedures have shown that the F_Q^T limit is not exceeded.

Measurements of the hot channel factors are required as part of startup physics tests, and whenever abnormal power distribution conditions require a reduction of core power to a level based on measured hot channel factors.

For normal operation, however, it is not necessary to measure F_Q and $F_{\Delta H}$ directly. Instead, it has been determined that, if the HBR 2 Technical Specification limits on control rod operation are met and the HBR 2 axial power distribution control procedures (given in terms of constant axial offset control) are observed, the above-stated hot channel factors will be met.

4.3.2.3 Reactivity Coefficients

The response of the reactor core to plant conditions or operator adjustments during normal operation, as well as the response during abnormal or accidental transients, is evaluated by means of a detailed plant simulation. In these calculations, reactivity coefficients are required to couple the response of the core neutron multiplication to the variables which are set by conditions external to the core. Since the reactivity coefficients change during the life of the core, a range of coefficients is established to determine the response of the plant throughout life and to establish the design of the Reactor Control and Protection System.

4.3.2.3.1 Fuel Temperature (Doppler) Coefficient

The Doppler coefficient is defined as the change in neutron multiplication per degree change in fuel temperature. The coefficient becomes slightly more negative with increasing fuel burnup.

As the fuel pellet temperature increases with power, the absorption in Uranium-238 increases due to Doppler broadening of the resonances. A large temperature drop occurs across the fuel pellet-clad gap. Under certain conditions, this gap may be closed, thus resulting in lower pellet temperature. The net effect is a lower effective fuel temperature, a higher Doppler coefficient, and a lower power coefficient than that which exists with a pellet-clad gap.

Calculations indicate the stability of the reactor to xenon oscillations is relatively insensitive to the thermal model used to obtain the power coefficient. The damping factor associated with the fuel Doppler effect is

$$\alpha_f = \frac{\partial K_{eff}}{\partial T} \frac{\partial T}{\partial P}$$

where: T = fuel temperature
P = power
K_{eff} = effective neutron multiplication factor

The quantity $\frac{\partial T}{\partial P}$ is larger for the gap model than for the no gap case but since the Doppler coefficient varies as $T^{-1/2}$ the term $\frac{\partial K_{eff}}{\partial T}$ is smaller. The net effect is that α_f is relatively insensitive to the thermal model in the range of power 0.5 to 1.5 of core average which is the range of interest for stability.

4.3.2.3.2 Moderator Coefficients

The moderator temperature coefficient in a core controlled by chemical shim is less negative than the coefficient in an equivalent rodded core. One reason is that control rods contribute a negative increment to the coefficient and in a chemical shim core, the rods are only partially inserted. Also, the chemical poison density is decreased with the water density upon an increase in temperature. This gives rise to a positive component in the moderator temperature coefficient due to boron being removed from the core. This is directly proportional to the amount of reactivity controlled by the dissolved poison.

The effect of burnup on the moderator temperature coefficient is calculated and the coefficient becomes more negative with increasing burnup. This is due to the buildup of plutonium and fission products and the dilution of the boric acid concentration with burnup. The latter effect is considerably more important. However, the buildup of equilibrium xenon contributes a positive increment to the coefficient for a constant boron concentration. With core burnup, the coefficient will become more negative as boron is removed because of a shift in the neutron energy spectrum due to the buildup of plutonium and fission products.

Similarly, burnable absorbers such as gadolinia provide a negative contribution to the moderator coefficient by offsetting some of the soluble boron in the core. The control rods provide a negative contribution to the moderator coefficient.

The moderator pressure coefficient has an opposite sign to the moderator temperature coefficient. The effect on the total coefficient is small because the pressure coefficient is 100 times smaller.

A uniform moderator density coefficient is defined as a change in the neutron multiplication per unit change in moderator density. The range of the moderator density coefficient from BOL to EOL is -0.1 to +0.3 $(\Delta k/k)/g/cm^3$.

4.3.2.3.3 Power Coefficient

In order to know the change in reactivity with power, it is necessary to know the change in the effective fuel temperature with power as well as the Doppler coefficient. It is very difficult to predict the effective temperature of the fuel using a conventional heat transfer model because of uncertainties in predicting the behavior of the fuel pellets. Therefore, an empirical approach is taken to calculate the power coefficient. The power coefficient becomes slightly more negative with increasing fuel burnup.

4.3.2.3.4 Comparison of Calculated and Experimental Reactivity Coefficients

Information on the verification of the neutronic design methods, by comparison to experimental data, is provided in Section 4.3.3 of the Updated FSAR.

4.3.2.3.5 Reactivity Coefficients Used in Transient Analysis

Reactivity coefficients used in the transient analysis of the HBR 2 reactor are provided in Chapter 15 of the Updated FSAR.

4.3.2.4 Control Requirements

Neutron-absorbing control rods provide reactivity control to compensate for more rapid variations in reactivity. The rods are divided into two categories according to their function. Some rods compensate for changes in reactivity due to variations in operating conditions of the reactor such as power or temperature. These rods comprise the control group of rods. The remaining rods, which provide shutdown reactivity, are termed shutdown rods. The total shutdown worth of all the rods is also specified to provide adequate shutdown with the most reactive rod stuck out of the core.

The difference between the control rod reactivity requirements at beginning and end of life and the installed worth of the control rods is available for excess shutdown upon reactor trip. The control rod requirements are discussed in the following sections.

4.3.2.4.1 Doppler

Control rods must be available to compensate for the reactivity change incurred with a change in power level due to the Doppler effect. The magnitude of this change has been established by correlating the experimental result of numerous operating cores as mentioned above.

4.3.2.4.2 Variable Average Moderator Temperature

The average temperature of the reactor coolant is increased with power level in the reactor. Since this change is actually a part of the power dependent reactivity change, along with the Doppler effect and void formation, the associated reactivity change must be controlled by rods. The largest amount of reactivity that must be controlled is at the end of life when the moderator temperature coefficient has its most negative value. By the end of the fuel cycle, the nonuniform axial depletion causes a severe power peak at low power. The reactivity associated with this peak is part of the power defect.

4.3.2.4.3 Redistribution

The control group is operated at full power within a prescribed band of travel in the core to compensate for periodic changes in boron concentration, temperature, or xenon. The band has been defined as the operational maneuvering band. When the rods reach either limit of the band, a change in boron concentration must be made to compensate for any additional change in reactivity, thus keeping the control group within the maneuvering band.

4.3.2.4.4 Void content

Void content in a pressurized water reactor (PWR) represents a relatively minor effect and is included as part of moderator temperature effects (see Section 4.3.2.4.2).

4.3.2.4.5 Rod insertion allowance

If sufficient boron is present in a chemically-shimmed core, the inherent operational control afforded by the negative moderator temperature coefficient is lessened to such a degree that the major control of transients resulting from load variations must be compensated for by control rods. The ability of the plant to accept major load variations is distinct from safety considerations, since the reactor would be tripped and the plant shut down safely if the rods could not follow the imposed load variations. In order to meet required reactivity ramp rates resulting from load changes, the control rods must be inserted a given distance into the core. The reactivity worth of this insertion has been defined as control rod bite.

The reactivity insertion rate must be sufficient to compensate for reactivity variation due to changes in power and temperature caused either by a ramp load change of fifteen percent per minute, or by a step load change of twenty percent. An insertion rate of 3×10^{-5} $\Delta k/k$ per second is adequate for the most adverse combinations of power and moderator coefficients. To obtain this minimum ramp rate one control bank of rods must remain slightly inserted into the core. The reactivity associated with this bite is less than 0.1 percent.

4.3.2.4.6 Burnup

Excess reactivity is installed at the beginning of each cycle to provide sufficient reactivity to compensate for fuel depletion and fission products throughout the cycle. This reactivity is controlled by the addition of soluble boron to the reactor coolant and by the use of burnable absorbers such as gadolinia. Since the excess reactivity for burnup is controlled by soluble boron, it is not included in control rod requirements.

The boron concentration must be limited during operating conditions to ensure the moderator temperature coefficient is negative. Burnable absorber rods can significantly reduce the actual boron concentration at start up, thus maintaining a negative moderator temperature coefficient.

4.3.2.4.7 Xenon and Samarium Poisoning.

Changes in xenon and samarium concentrations in the core occur at a sufficiently slow rate, even following rapid power level changes, that the resulting reactivity change is controlled by changing the soluble boron concentration.

4.3.2.4.8 pH Effects

Changes in reactivity due to a change in coolant pH, if any, are sufficiently small in magnitude and occur slowly enough to be controlled by the boration system.

4.3.2.4.9 Experimental Confirmation

Information on the experimental confirmation of control requirement calculational methods is discussed in Section 4.3.3 of the Updated FSAR.

4.3.2.4.10 Control

Core reactivity is controlled by means of a chemical poison dissolved in the reactor coolant and RCC assemblies, as described below.

4.3.2.4.11 Chemical Poison

Boron in solution as boric acid is used to control relatively slow reactivity changes associated with:

a) The moderator temperature defect in going from cold shutdown at ambient temperature to a constant moderator temperature at equilibrium no-load value

b) The transient xenon and samarium poisoning, such as that following power changes or changes in RCC position, and

c) The excess reactivity required to compensate for the effects of fissile inventory depletion and buildup of long-life fission products.

4.3.2.4.12 RCC Assemblies

Full length RCC assemblies are employed. The full length RCC assemblies are used for shutdown and control purposes to offset fast reactivity changes associated with:

a) The required shutdown margin in the hot zero power, stuck rods condition.

b) The reactivity compensation as a result of an increase in power above hot zero power (power defect including Doppler and moderator reactivity changes).

c) Unprogrammed fluctuations on boron concentration, reactor coolant temperature, or xenon concentration (with rods not exceeding the allowable rod insertion limits).

d) Reactivity ramp rates resulting from load changes.

4.3.2.4.13 Reactor Coolant Temperature

Reactor coolant (or moderator) temperature control has added flexibility in reactivity control of the reactor. This feature takes advantage of the negative moderator temperature coefficient inherent in a pressurized water reactor to:

a) Maximize return to power capabilities

b) Provide power load regulation capabilities without requiring control rod compensation, and

c) Extend the time in cycle life during which daily load follow operations can be accomplished.

Reactor coolant temperature control supplements the dilution capability of the plant by lowering the reactor coolant temperature to supply positive reactivity through the negative moderator coefficient of the reactor. After the transient is over, the system recovers the reactor coolant temperature to the programmed value.

Moderator temperature control of reactivity, like soluble boron control, has the advantage of not significantly affecting the core power distribution.

4.3.2.4.14 Peak Xenon Buildup

Compensation for the peak xenon buildup is accomplished using the Chemical Shim Control System. Startup from the peak xenon condition is accomplished with a combination of rod motion and boron dilution. The boron dilution may be made at any time, including during the shutdown period, provided the shutdown margin is maintained.

4.3.2.4.15 Load Follow Control and Xenon Control

During load follow maneuvers, power changes are accomplished using control rod motion and dilution or boration by the Chemical Shim Control System, as required. Control rod motion is limited by the control rod insertion limits on the control rods as provided in the Technical Specifications. The power distribution is maintained within acceptable limits through location of the control rod bank. Reactivity changes due to the changing xenon concentration can be controlled by rod motion and/or changes in the soluble boron concentration.

Late in cycle life, extended load follow capability is obtained by augmenting the limited boron dilution capability at low soluble boron concentrations by temporary moderator temperature reductions.

Rapid power increases from partial power levels during load follow operations are accomplished with a combination of rod motion, moderator temperature reductions, and boron dilution. Compensation for the rapid power increase is accomplished initially by a combination of rod withdrawal and moderator temperature reduction. As the slower boron dilution takes effect after the initial rapid power increase, the moderator temperature returns to the programmed value.

4.3.2.5 Control Rod Patterns and Reactivity Worth

The control rod patterns are provided in Figure 4.3.2-1.

4.3.2.6 Stability

Reactors of the size of HBR have been demonstrated to be unstable with respect to axial xenon oscillations, and such oscillations have been observed at HBR. From an operations standpoint, however, the control of xenon oscillations has not presented any significant problems, although there have been instances where a temporary reduction in power was necessary in order to cope with the problem.

The control aspects of a xenon oscillation closely tie in with the core Technical Specifications on power peaking and allowable axial offset considerations. Since these Technical Specifications may change with respect to future operation of the plant, detailed analysis of the xenon oscillation phenomenon has not been carried out.

Figure 4.3.2-2 displays the results of a xenon oscillation performed with the three-dimensional XTG model. The calculations were stopped 40 hr beyond the time of the initiation of the transient, as this particular oscillation appeared to be damped. The core was perturbed by reducing power to 50 percent of rated combined with a D-bank insertion to 140 steps. The core was left in this condition for 8 hr at which time the power and the D-bank insertion both were returned to their original levels. The subsequent oscillation was calculated using 0.5 hr time steps. The cycle burnup was 8,000 MWD/MTU. Another calculation was initiated earlier in the cycle but, as was expected, this oscillation was even more damped and analysis was terminated.

There are primarily two effects that contribute to the nature of the oscillation. The first is the "flatness" of the axial power distribution and the second is the highly negative moderator temperature coefficient. Both of these effects are more prevalent toward the EOC and contribute toward instability of the core with respect to xenon oscillation.

4.3.3 Analytical Methods

The neutronic calculational methods utilized to support reactor core design and operation are summarized in the following sections. The methodology has been reviewed and approved for generic application to pressurized water reactors of Westinghouse design.

4.3.3.1 Design Methodology

A consistent set of well formulated analytical methods and techniques is essential to assure reliability of the neutronic design of reload cores. Based on continuing comparisons with operating data and resultant model refinements, a neutronics design methodology has evolved which utilizes a combination of 2-D and 3-D core representations. The methodology used in the reload core analyses is described in References 4.3.3-17 and 4.3.3-18.

The basic nuclear parameters, including the gadolinia-bearing pins, are calculated with the CASMO-3 code. Assembly-average macroscopic cross-sections in two energy groups are obtained from CASMO-3 as a function of assembly exposure. Microscopic cross-sections for boron and xenon are also obtained from CASMO-3.

Calculations are done in three dimensions incorporating sixteen axial nodes (within the active fuel height) with the PRISM reactor code (Reference 4.3.3-18). With this reactor model, axial effects, including predicted values of F^N_Q, $F_{\Delta H}$, F_{xy}, and F_Z, can be studied. Thermal-hydraulic feedback and axial exposure distribution effects on power shapes, rod worths, and cycle lifetime are explicitly included in the analysis.

4.3.3.2 Nuclear Measurement Uncertainty

Full core measured power distributions must be periodically determined in nuclear reactors. The power distribution is determined through the use of measured and calculated data, and hence contains a degree of uncertainty. The analysis of the uncertainty in the measured power distribution applicable to H.B. Robinson Unit 2 is addressed in the generic uncertainty for Westinghouse PWRs using AREVA Inc. methods (References 4.3.3-17).

The data for the analysis were obtained from a spectrum of Westinghouse pressurized water reactors. Several cycles of operating data and power distribution measurements were utilized from each plant. Measured data for assembly local power distributions were also obtained from critical experiments performed by Babcock and Wilcox. The uncertainty analyses have been approved by the NRC for application to Westinghouse type PWRs.

4.3.3.3 Power Distribution Control Procedures

The control of the core power distribution is accomplished by following the procedures in Reference 4.3.3-12. These procedures, denoted PDC-3, have been approved by the NRC for application to H. B. Robinson Unit 2. With PDC-3 the core axial flux difference measured with the excore neutron detectors is maintained within specified bounds to assure that the core power peaking remain within allowable limits.

The significant feature of the PDC-3 procedure is that it focuses on the variation in the axial power distribution rather than the axial power distribution itself. The periodically measured $F_Q(z)$ power distribution in the core is utilized as a basis for the analysis of potential power distributions allowed by the procedure. The maximum variation in the power peaking distribution is determined based on the allowed variation in the flux difference about the measured target flux difference. This variation in power peaking distribution is added to the target $F_Q(z)$ power peaking distribution measured periodically at the plant. The results are then compared to the power peaking distribution limit to demonstrate that the limit is not exceeded.

4.3.3.4 Rod Ejection Analysis

A Control Rod Ejection Accident is defined as the mechanical failure of a control rod mechanism pressure housing, resulting in the ejection of a Rod Cluster Control Assembly (RCCA) and drive shaft. The consequence of this mechanical failure is a rapid reactivity insertion together with an adverse core power distribution, possibly leading to localized fuel rod damage.

The rod ejection accident has been evaluated with the procedures developed in the ENC Generic Rod Ejection Analysis, Reference 4.3.3-13, which has been generically approved by the NRC for use in PWR cores. The ejected rod worths and hot pellet peaking factors are calculated using the PRISM code. No credit is taken for the power flattening effects of Doppler or moderator feedback in the calculation of ejected rod worths or resultant peaking factors. The other significant neutronics parameters are the core average delayed neutron fraction and the Doppler temperature coefficient. These important neutronics parameters are correlated and the pellet energy deposition resulting from an ejected rod is conservatively evaluated explicitly for BOC and EOC conditions.

REFERENCES: SECTION 4.3

4.3.3-1 Deleted by Revision No. 17.

4.3.3-2 Deleted by Revision No. 17.

4.3.3-3 Deleted by Revision No. 17.

4.3.3-4 Deleted by Revision No. 17.

4.3.3-5 Deleted by Revision No. 15

4.3.3-6 Deleted by Revision No. 15

4.3.3-7 Deleted by Revision No. 25

4.3.3-8 Deleted by Revision No. 15

4.3.3-9 Deleted by Revision No. 15

4.3.3-10 Deleted by Revision No. 14

4.3.3-11 Deleted by Revision No. 14

4.3.3-12 ANF-88-054(P)(A), "PDC-3: Advanced Nuclear Fuels Corporation Power Distribution Control for Pressurized Water Reactors and Application of PDC-3 to H. B. Robinson Unit 2," Advanced Nuclear Fuels Corporation, October 1990.

4.3.3-13 XN-NF-78-44(NP)(A), "A Generic Analysis of the Control Rod Ejection Transient for Pressurized Water Reactors", Exxon Nuclear Company, October 1983.

4.3.3-14 Deleted by Revision No. 15

4.3.3-15 Deleted by Revision No. 17.

4.3.3-16 Deleted

4.3.3-17 EMF-93-164(P)(A), "Power Distribution Measurement Uncertainty for INPAX-W in Westinghouse Plants, "Siemens Power Corporation, February 1995, transmitted to NRC by letter dated February 13, 1995.

4.3.3-18 EMF-96-029(P)(A), Volumes 1 and 2, "Reactor Analysis System for PWR's Volume 1 – Methodology Description, Volume 2 – Benchmarking Results," Siemens Power Corporation, January 1997.

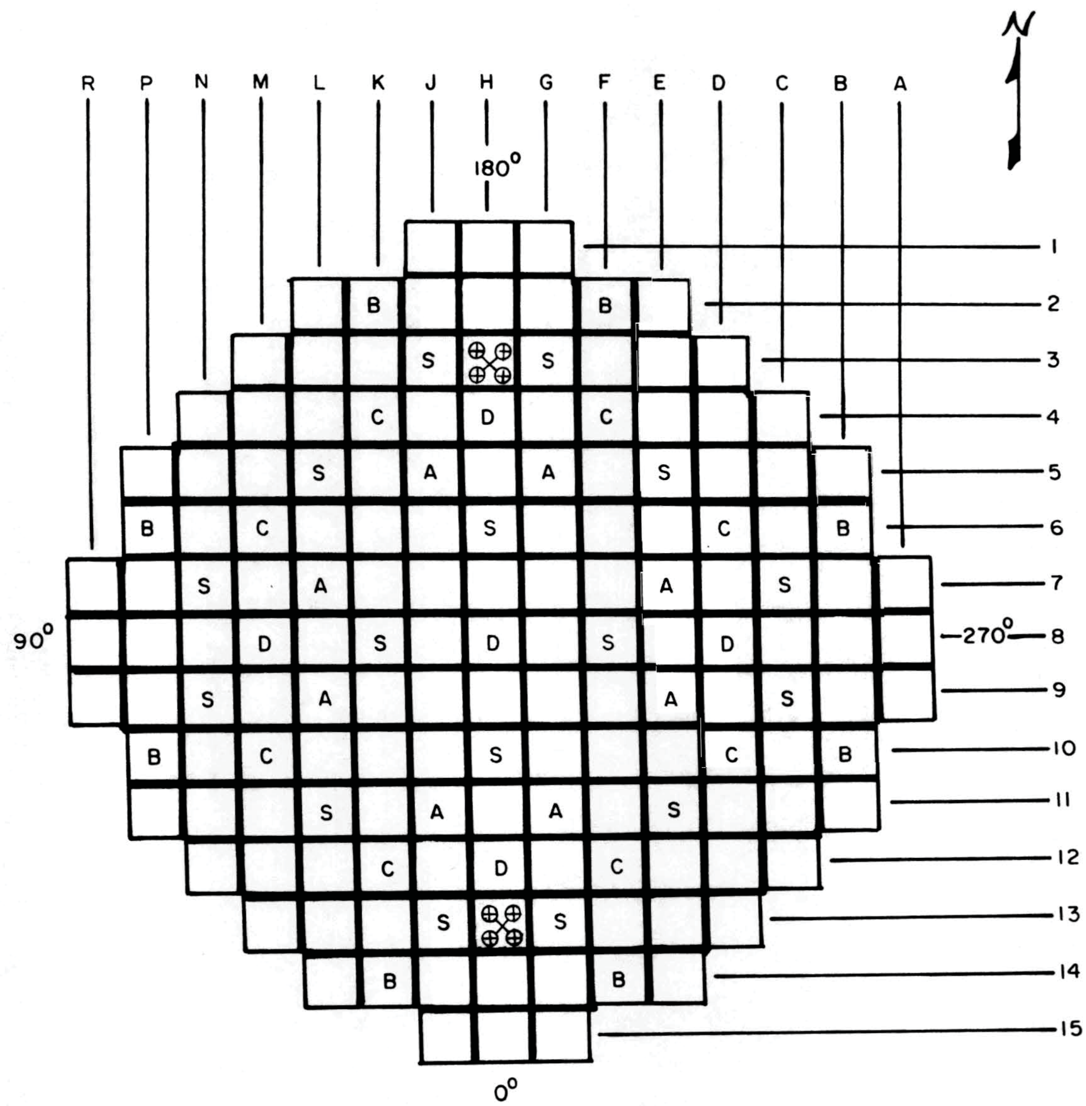

CONTROL ROD CLUSTER GROUPS

CONTROL GROUP 1	(A)	8
CONTROL GROUP 2	(B)	8
CONTROL GROUP 3	(C)	8
CONTROL GROUP 4	(D)	5
SHUTDOWN	(S)	16
	TOTAL	45

= SECONDARY SOURCE ASSEMBLY LOCATIONS (LOCATIONS MAY OR MAY NOT CONTAIN A SOURCE ASSEMBLY)

AMENDMENT 3

H. B. ROBINSON UNIT 2 Carolina Power & Light Company UPDATED FINAL SAFETY ANALYSIS REPORT	PATTERN OF CONTROL ROD CLUSTER GROUPS AND SOURCE ASSEMBLY LOCATIONS	FIGURE 4.3.2 - 1

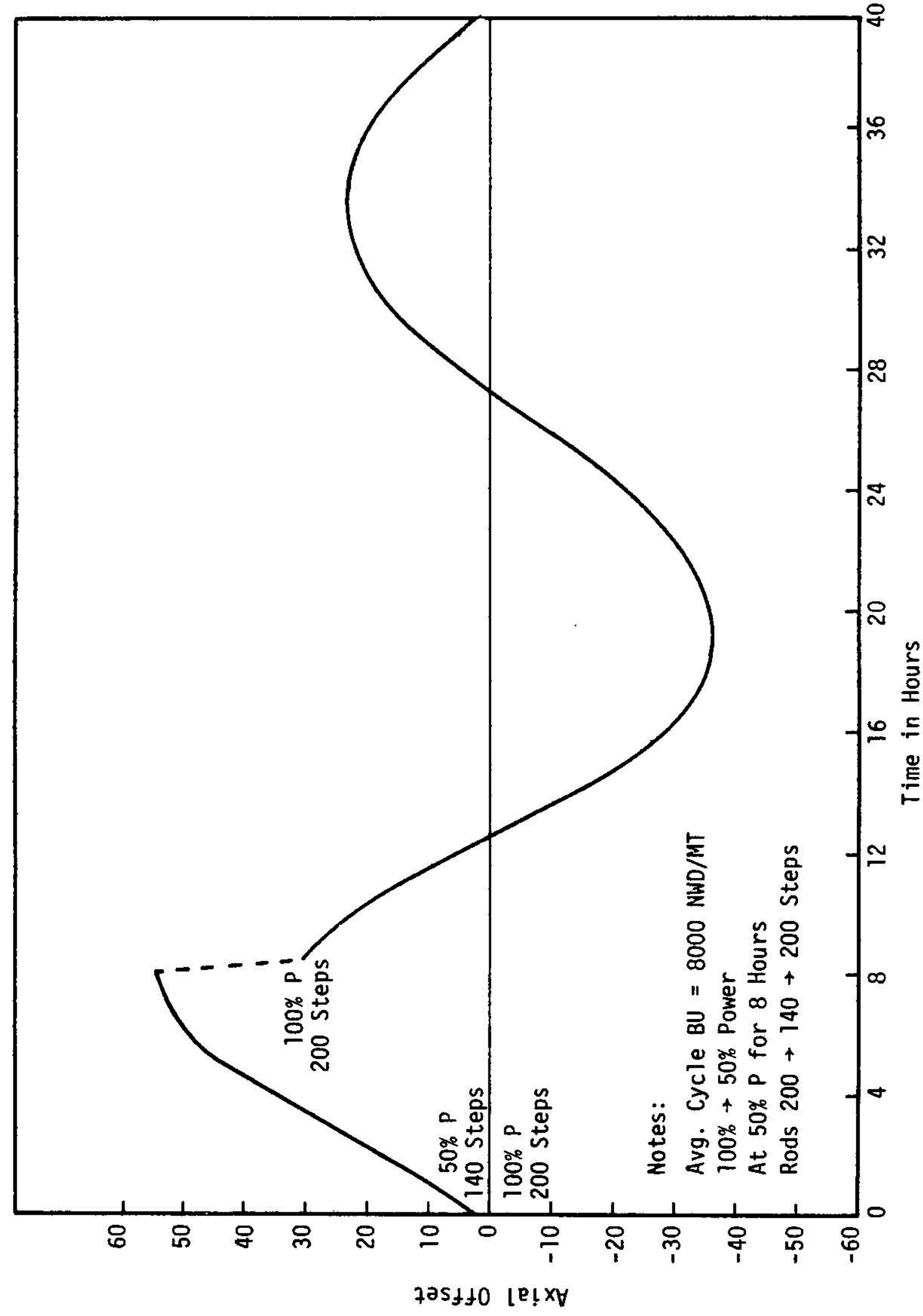

H. B. ROBINSON UNIT 2 Carolina Power & Light Company UPDATED FINAL SAFETY ANALYSIS REPORT	H. B. ROBINSON UNIT 2 - CYCLE 4 AXIAL XENON OSCILLATION AXIAL OFFSET vs. TIME	FIGURE 4.3.2 - 2

4.4 THERMAL AND HYDRAULIC DESIGN

4.4.1 DESIGN BASIS

The following sections discuss the thermal-hydraulic design bases for the reactor core. Chapter 5 of the Updated FSAR contains a description of the design bases for the reactor coolant system (RCS).

4.4.1.1 Departure From Nucleate Boiling Design Basis

To maintain fuel rod integrity and prevent fission product release, it is necessary to prevent clad overheating under all operating conditions. This is accomplished by preventing a departure from nucleate boiling (DNB). DNB would cause a large decrease in the heat transfer coefficient between the fuel rods and the reactor coolant resulting in high clad temperatures.

The HBR 2 reactor core is designed so that the minimum calculated DNB ratio during normal operation, including anticipated transients, is greater than or equal to the safety limit specified in Section 4.4.2.1.

4.4.1.2 Fuel Temperature Design Basis

The reactor core is designed such that no fuel melts during normal operation, including anticipated transients.

4.4.2 Description

The following sections describe the thermal-hydraulic design of the reactor core. Chapter 5 of the Updated FSAR contains a description of the thermal-hydraulic design of the RCS.

4.4.2.1 Definition of Departure from Nucleate Boiling (DNB) Ratio

The ratio of the heat flux causing DNB at a particular core location to the existing heat flux at the same core location, is the DNB ratio. A DNB ratio equal to the safety limit corresponds to a 95 percent probability at a 95 percent confidence level that DNB does not occur. This value is chosen as the margin to DNB for all operating conditions.

DNB is not, however, an observable parameter during reactor operation. Therefore, the observable parameters, reactor power, reactor coolant temperature and reactor coolant pressure have been related to DNB through the DNB correlation. The HTP correlation for High Thermal Performance (HTP™) fuel has a DNBR safety limit of 1.141 (Reference 4.4.2-3). Curves presented in the HBR 2 Technical Specifications represent the loci of points of reactor power, reactor coolant pressure and inlet temperature for which the DNB ratio is less than the safety limit. The area of safe operation is the lower inlet temperature and higher reactor coolant pressures limited by one specified curve of the reactor power parameter family of curves shown. The parameters used in the development of the curves are checked in the course of plant startup tests, and the curves are modified if necessary.

4.4.2.2 Hot Channel Factors

The enthalpy rise factors are thermal-hydraulic performance indicators. These factors indicate the effect on the enthalpy rise in the hot subchannel resulting from the geometry and components of the AREVA Inc. fuel design. Each of the enthalpy rise factors was developed from the results of the thermal-hydraulic calculations. The DNB methodology using the XCOBRA-IIIC computer code is described in Reference 4.4.2-1.

4.4.2.2.1 Engineering enthalpy rise factor

Because of tolerances in the manufacture of the fuel, in particular variations from the nominal design values of pellet density, pellet diameters, and enrichment over the active length, the local heat flux in the highest enthalpy rise subchannel could have been higher than nominal by three percent (engineering heat flux factor). The engineering enthalpy rise factor was evaluated by XCOBRA-IIIC computer runs with and without the three percent increase in local heat flux for the hottest fuel rod adjacent to the high enthalpy rise subchannel.

4.4.2.2.2 Inlet plenum maldistribution factor

The inlet plenum maldistribution is a reactor vessel characteristic that is specified in the HBR FSAR to be " 5 percent. To assume a 5 percent increase in enthalpy rise in the hot subchannel would be overly conservative because of the effects of subchannel turbulent and cross flow mixing which tend to neutralize this inlet flow situation at the point of MDNBR. Because of the effects of turbulent and crossflow mixing, the enthalpy rise factor resulting from a "5 percent inlet flow maldistribution is unaffected.

4.4.2.2.3 Flow mixing enthalpy rise factor

The enthalpy rise factor in the hot channel is adjusted for turbulent mixing in the XCOBRA III-C code. The turbulent mixing model is the ROWE-ANGLE model. See Reference 4.4.2-4.

4.4.2.2.4 Flow redistribution

The enthalpy in the hot subchannel is increased by flow diversion resulting from the higher frictional losses which result from subcooled nucleate boiling. The flow that is diverted from the hot subchannel due to the effect of subcooled voiding was found to cause a significant increase in the enthalpy rise.

4.4.3 Instrumentation Requirements

The following sections describe the instrumentation requirements for the reactor core. Chapter 5 of the Updated FSAR contains a description of the instrumentation requirements for the RCS.

4.4.3.1 Incore Instrumentation

The incore instrumentation system consists of 46 dual element bottom-mounted (one element is a spare thermocouple) thermocouples, positioned to measure fuel assembly coolant outlet temperature at preselected locations; and 46 flux thimbles, which run the length of selected fuel assemblies for measurement of the neutron flux distribution within the core. Five movable miniature neutron flux detectors with associated control and readout equipment may be used to scan the length of selected fuel assemblies to provide remote reading of the axial flux distribution. The incore instrumentation system is shown in Figure 4.4.3-1.

The experimental data obtained from the incore temperature and flux distribution instrumentation system, in conjunction with previously determined analytical information, can be used to determine the fission power distribution in the core at any time throughout core life. Once the fission power distribution has been established, the maximum power output is primarily determined by thermal power distribution and the thermal and hydraulic limitations, which determine the maximum core capability.

The incore instrumentation provides information that may be used to calculate the coolant enthalpy distribution, the fuel burnup distribution, and to estimate the coolant flow distribution.

4.4.3.2 Overtemperature and Overpower ΔT Instrumentation

The overpower ΔT reactor trip prevents power density anywhere in the core from exceeding the fuel power density corresponding to fuel centerline melt and includes corrections for axial power distribution, change in density, and heat capacity of water with temperature, and dynamic compensation for piping delays from the core to the loop temperature detectors. The specified setpoints meet this requirement and include allowance for instrument errors.

The overpower and overtemperature protection system setpoints have been revised to include effects of fuel densification and the increase in rated thermal output to 2339 MWt on core safety limits. The revised setpoints in the Technical Specifications ensure the combination of power, temperature, and pressure will not exceed the core safety limits shown in Figure 4.4.3-2.

4.4.3.3 Instrumentation to Limit Maximum Power Output

The Reactor Control and Protection System is designed to prevent any anticipated combination of transient conditions for Reactor Coolant System (RCS) temperature, pressure, and thermal power level that would result in a DNB ratio of less than the safety limit (specified in Section 4.4) based on steady state nominal operating power levels less than or equal to 100 percent, steady state nominal operating RCS average temperature less than or equal to 575.9°F, and a steady state nominal operating pressure of 2235 psig. Allowances are made in the initial conditions and in the transient analyses to account for an uncertainty in power due to the calorimetric, a 40 psi uncertainty in pressure and operation at the minimum flow and maximum power peaking allowed by the Technical Specifications. Sufficient conservatism exists in the transient methodology to accommodate the variation in the initial RCS temperature allowed by the Technical Specifications. The combined effect of these allowances is verified for anticipated transients to confirm that the minimum DNB ratio remains above the safety limit and by demonstrating that the OTΔT trip will preclude DNB for slow transients in temperature, pressure and power with at least a 95% probability at a 95% confidence level.

4.4.3.4 Core Subcooling Monitor

The purpose of the subcooling monitor is to provide a continuous indication of margin to saturated conditions. The monitor uses inputs from core outlet thermocouples, RCS hot and cold leg resistance temperature detectors and RCS system pressure to drive a micro-processor which calculates saturation temperature and determines the margin to saturation based on the inputs. The individual inputs as well as the margin to saturation can be displayed on the monitor's plasma display panel. The monitor has 2 independent channels, and each channel has its own plasma display panel.

4.4.3.5 Digital Metal Impact Monitoring System

The Digital Metal Impact Monitoring System (DMIMS) uses an array of accelerometers externally mounted to the major components to the reactor system, signal conditioning equipment, recording and alarm equipment, and diagnostic equipment and software. This system collects information that may be used by the operator in the detection, location, and identification of loose parts within the reactor coolant system.

4.4.3.5.1 Design Basis

The system components of the DMIMS within the containment are designed and installed to function following all seismic events that do not require plant shutdown (i.e., up to and including OBE). Recording equipment need not function without maintenance following the specified seismic event provided the audio or visual alarm capability remains functional.

The system is designed to facilitate the maintenance and repair of malfunctioning components with minimum occupational radiation exposure.

4.4.3.5.2 System Description

There are ten (10) loose parts monitoring sensors (accelerometers) located in pairs to provide for sensor redundancy. Sensors are provided at the reactor vessel head lug, the reactor vessel bottom, and at each steam generator primary and secondary side.

Instrumentation channel components (including cabling and preamplifiers) associated with the sensors at each location are physically separated up to a point in the plant that is always accessible for maintenance during full power operation.

The system alert level established during preoperational testing includes the effects of background noise. This alert level incorporates suitable internal criteria to distinguish transient signals caused by the impact of loose parts from the transient pulse signal associated with normal hydraulic, mechanical, electrical noise, etc. The false alert signals resulting from plant maneuvers, such as control rod stepping, reactor trip, reactor coolant pump starts, etc., will be avoided either by automatic procedures that momentarily override actuation of the alert level alarm or by administrative procedures that are used by the control room operator. When the alert level is exceeded, a visual or audible alarm alerts the control room operator of that condition. The data acquisition system may be used to record all DMIMS signal wave forms.

Upon detection of loose parts, an alarm is indicated on the DMIMS panel. The event recorder (printer) provides a hard copy of an event that resulted in alarm condition on request. At the end of each day, the DMIMS automatically provides a printout of the day's activity regardless of alarm conditions. The FM tape recorder provides historical data for diagnostic purposes and can be manually or automatically started.

REFERENCES: SECTION 4.4

4.4.2-1 XN-NF-82-21 (P)(A), Revision 1, "Application of Exxon Nuclear Company PWR Thermal Margin Methodology to Mixed Core Configuration," September 1983.

4.4.2-2 Deleted by Revision No. 14

4.4.2-3 EMF-92-153(P)(A), Revision 1, "HTP: Departure From Nucleate Boiling Correlation for High Thermal Performance Fuel," January 2005.

4.4.2-4 XN-NF-75-21(P)(A) Revision 2, "XCOBRA-IIIC: A Computer Code to Determine the Distribution of Coolant during Steady State and Transient Core Operation," Exxon Nuclear Company, January 1986.

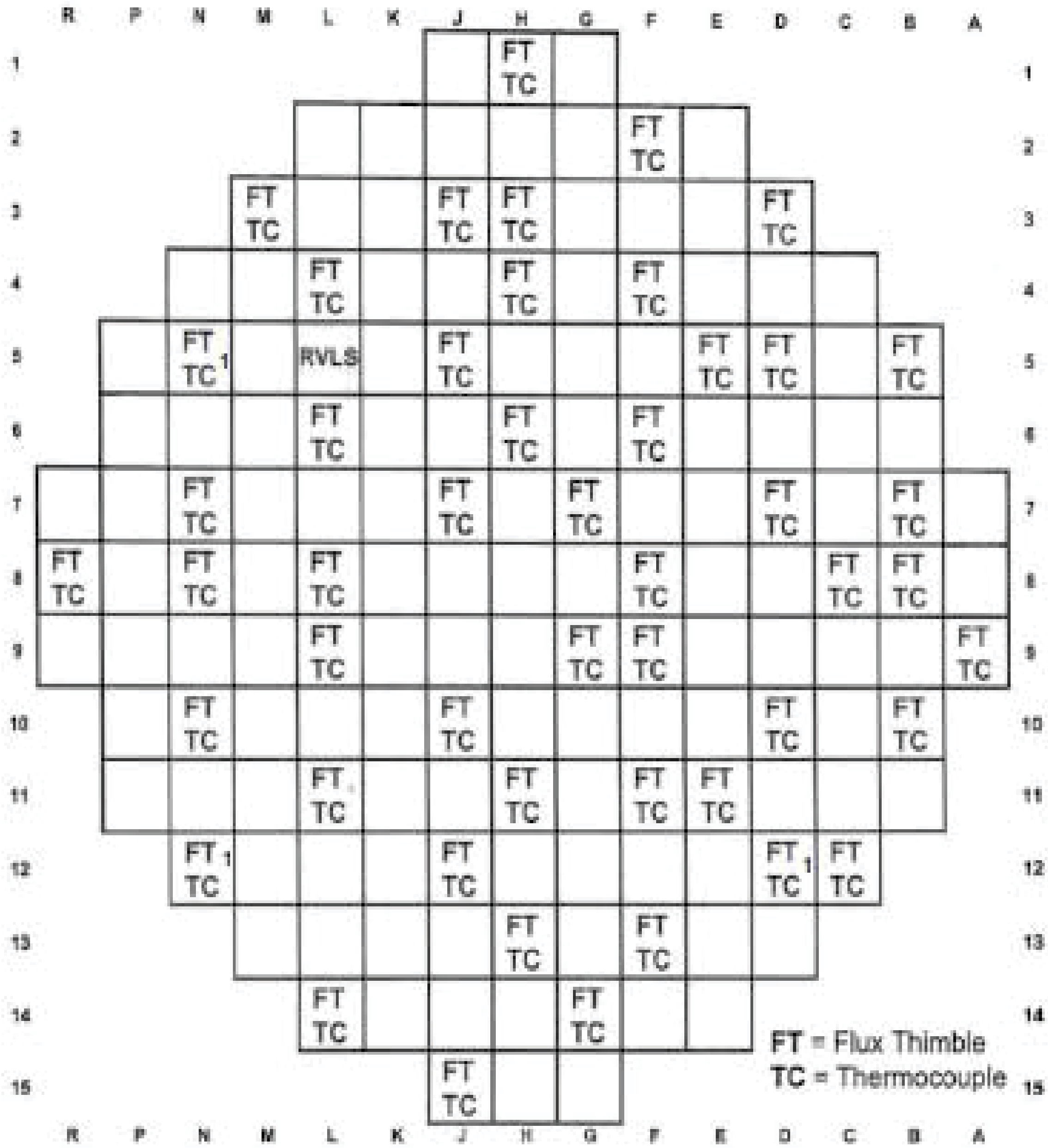

Note 1: The Flux Thimbles and Thermocouples in Core positions N-05, N-12, and D-12 are abandoned and cannot be used.

Revision No. 25

H. B. Robinson Unit 2 Carolina Power & Light Company UPDATED FINAL SAFETY ANALYSIS REPORT	X-Y View of H. B. Robinson Core	FIGURE No. 4.4.3-1

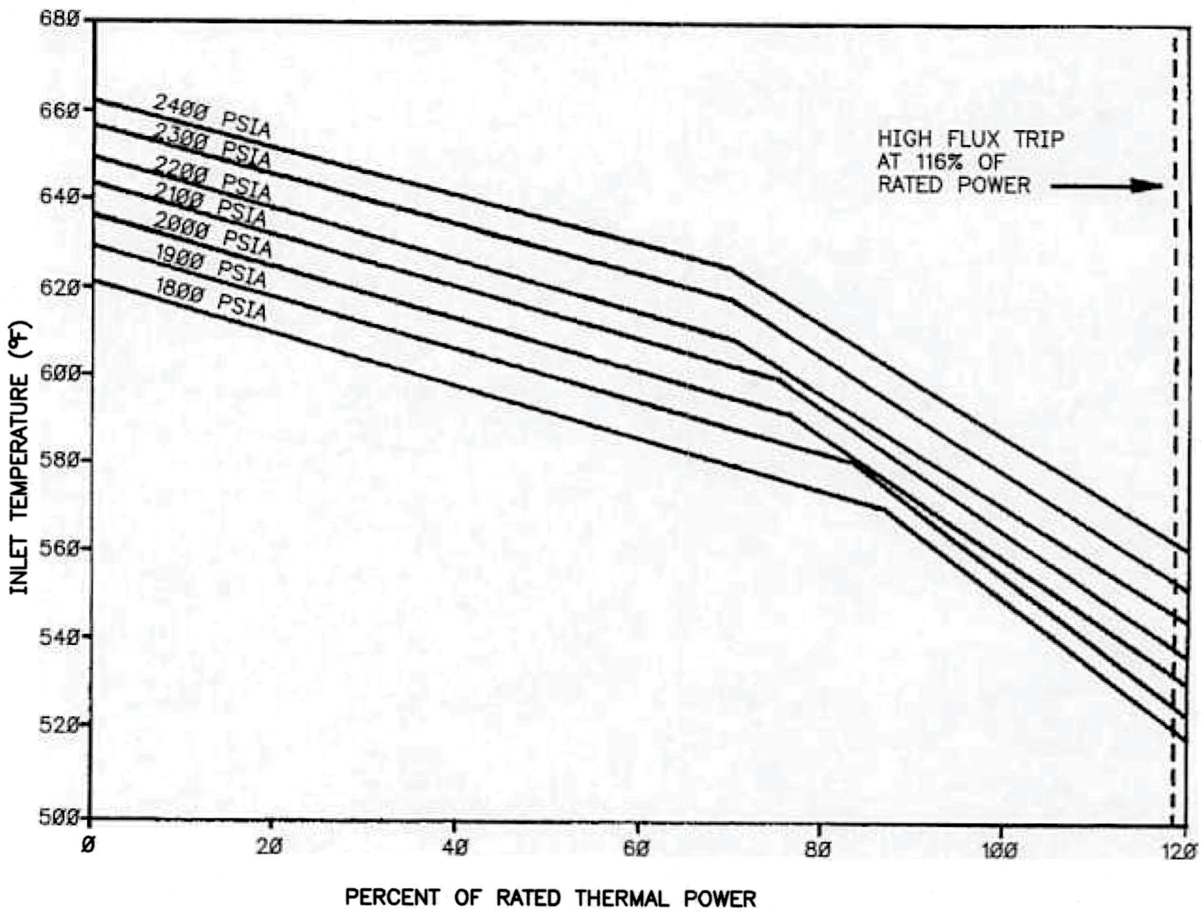

Revision No. 19

H.B. ROBINSON UNIT 2 Carolina Power & Light Company UPDATED FINAL SAFETY ANALYSIS REPORT	CORE PROTECTION BOUNDARIES – FOR 3 LOOP OPERATION	FIGURE 4.4.3–2

4.5 REACTOR MATERIALS

4.5.1 CONTROL ROD DRIVE SYSTEM STRUCTURAL MATERIALS

The control rod drive (CRD) system is described in Section 3.9.4 and consists of the CRD mechanism to the coupling interface with the control rod. The structural materials for the major components exclusive of the electrical components are discussed below.

All parts exposed to reactor coolant, such as the pressure vessel, latch assembly and drive rod, are made of metals which resist the corrosive action of the water. Three type of metals are used exclusively: stainless steels, Inconel X, and cobalt based alloys. Wherever magnetic flux is carried by parts exposed to the reactor coolant, stainless steel is used. Cobalt based alloys are used for the pins and latch tips.

Inconel X is used for the springs of both latch assemblies and SA-182 Grade F316 Stainless Steel is used for the latch housings. Hard chrome plating provides wear surfaces on the sliding parts and prevents galling between mating parts (such as threads) during assembly.

Outside of the pressure vessel, where the metals are exposed only to the reactor plant containment environment and cannot contaminate the reactor coolant, carbon and stainless steels are used. Carbon steel, because of its high permeability, is used for flux return paths around the operating coils. It is zinc plated 0.001 in. thick to prevent corrosion.

4.5.2 REACTOR INTERNALS MATERIAL

The reactor internal description, design bases, and structural analyses are given in Section 3.9.5. The thermal shield, upper and lower internal support assemblies, core barrel, and other reactor internals are made of ASTM A-240, Type 304 Stainless Steel.

4.6 FUNCTIONAL DESIGN OF REACTIVITY CONTROL SYSTEMS

Each control rod drive assembly is designed as a hermetically sealed unit to prevent leakage of reactor coolant water. All pressure containing components are designed to meet the requirements of the ASME code, Section III, Nuclear Vessels for Class A vessels.

The control rod drive assemblies for the full length rods provide rod cluster control (RCC) assembly insertion and withdrawal rates consistent with the required reactivity changes for reactor operational load changes. This rate is based on the worths of the various rod groups, which are established to limit powerpeaking flux patterns to design values. The maximum reactivity addition rate is specified to limit the magnitude of a possible nuclear excursion resulting from a control system or operator malfunction.

Also, the control rod drive assemblies for the full length rods provide a fast insertion rate during a "trip" of the RCC assemblies which results in a rapid shutdown of the Reactor Coolant System. This rate is based on the results of various reactor emergency analyses, including instrument and control delay times and the amount of reactivity that must be inserted before deceleration of the RCC assembly occurs.

Additional information on the control rod drives is contained in Section 3.9.